



저작자표시-비영리-변경금지 2.0 대한민국

이용자는 아래의 조건을 따르는 경우에 한하여 자유롭게

- 이 저작물을 복제, 배포, 전송, 전시, 공연 및 방송할 수 있습니다.

다음과 같은 조건을 따라야 합니다:



저작자표시. 귀하는 원저작자를 표시하여야 합니다.



비영리. 귀하는 이 저작물을 영리 목적으로 이용할 수 없습니다.



변경금지. 귀하는 이 저작물을 개작, 변형 또는 가공할 수 없습니다.

- 귀하는, 이 저작물의 재이용이나 배포의 경우, 이 저작물에 적용된 이용허락조건을 명확하게 나타내어야 합니다.
- 저작권자로부터 별도의 허가를 받으면 이러한 조건들은 적용되지 않습니다.

저작권법에 따른 이용자의 권리는 위의 내용에 의하여 영향을 받지 않습니다.

이것은 [이용허락규약\(Legal Code\)](#)을 이해하기 쉽게 요약한 것입니다.

[Disclaimer](#)

Master Thesis of the University of Ulsan

**Design and Optimization of Conformal Cooling
Channels for Increasing Cooling Efficiency in Injection
Molding**

Department of Mechanical and Automotive Engineering

University of Ulsan

Ulsan, Korea

Wang Yuandi

2023

**Design and Optimization of Conformal Cooling
Channels for Increasing Cooling Efficiency in Injection
Molding**

Supervisor: Prof. Chang-Myung Lee

Author: Wang Yuandi

**Department of Mechanical and Automotive Engineering
University of Ulsan**

**A dissertation submitted to the faculty of the University of Ulsan
in partial fulfillment the requirement for the degree of Master of
Philosophy in the Department of Mechanical and Automotive
Engineering.**

Ulsan, Korea

Jun. 12nd, 2023

Approved by

Professor Chang-Myung Lee

Wang Yuandi 의 공학박사학위 논문을 인준함

심사위원장 임옥택

(인) 

심사위원 이병룡

(인) 

심사위원 이장명

(인) 

울산대학교 대학원

2023 년 06 월


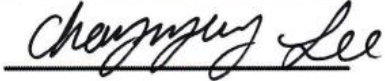

**To Approve the Submitted Dissertation for the Degree of
Master of Science in Mechanical and Automotive Engineering**

By

Wang Yuandi

**Title: Design and Optimization of Conformal Cooling Channels for
Increasing Cooling Efficiency in Injection Molding**

June 2023

| | | |
|----------------------------------|---------------------------------|--|
| Committee Chair Professor | OckTaeck Lim |  |
| Committee | Professor ChangMyung Lee |  |
| Committee | Professor ByungRyong Lee |  |

Graduate School

University of Ulsan, South Korea

ABSTRACT

The study establishes a mathematical model to analyze the heat transfer in injection molds and investigates the factors that influence cooling time and temperature distribution. Analysis of variance and response surface methodology are employed to examine the impact of geometrical parameters of the cooling channels. The NSGA-II multi-objective optimization algorithm is then applied to optimize the conformal cooling channels for products with varying wall thicknesses, resulting in Pareto optimal solutions for the channel design parameters. For plastic products with a wall thickness less than 2 mm, the diameter of the conformal cooling channels (d) is set to 4 mm, the distance between adjacent channel centerlines (l) is set to 8 mm, and the distance from the channel center to the cavity surface (s) is set to 6 mm. For wall thickness between 2-4mm, $d = 8\text{mm}$, $l = 16\text{mm}$, $s = 12\text{mm}$. For wall thickness between 4-6mm, $d = 12.5\text{mm}$, $l = 24\text{mm}$, $s = 18\text{mm}$. The simulation results demonstrate that the implementation of conformal cooling channels can reduce cooling time by 30% compared to traditional channels. Furthermore, the uniformity of temperature distribution across the entire plastic product is improved, leading to high-quality of products.

Key words: Conformal Cooling Channel; Injection Molding;
Multi-objective optimization; Response Surface Methodology;
NSGA-II

ACKNOWLEDGEMENTS

As this dissertation is completed, I would like to express my sincere gratitude to the people who helped me during my graduate studies; without their help, I would not have been able to complete this dissertation.

I am incredibly grateful to my advisor Professor Chang-Myung Lee and Professor Hong-Seok Park, for their help and guidance during my master's studies. The support of Professor Lee is the most significant driving force in my master's study, and this learning experience will benefit me for a lifetime. Their rigorous work attitude, extensive and solid theoretical foundation and diligent work style have left a deep impression on me. Also, I would like to thank other kind professors who have taught me in the Department of Mechanical and Automotive Engineering.

At the same time, I would like to thank the other students of University of Ulsan, who provided rich opinions, ideas and directions for my research and life. They gave me a lot of help when I was in difficulty. When I had questions, I explained them carefully. They provided a lot of help for the completion of my project. I really appreciate them.

I would like to thank my friends from China, Ge Cao, Yu Shen, Zhengtong Shan, for their help. They gave me unforgettable friendships and helped me while studying abroad. We spent a fulfilling and enjoyable time together at the school. I sincerely thank my families, for their unlimited support, understanding, encouragement and patience during my study and life. Thanks for everything in my life.

TABLE OF CONTENTS

| | |
|--|-----|
| ABSTRACT | i |
| ACKNOWLEDGEMENTS | ii |
| TABLE OF CONTENTS | iii |
| LIST OF FIGURES | vii |
| LIST OF TABLE | ix |
| ABBREVIATIONS | xi |
| INTRODUCTION | 1 |
| 1.1 Research background | 1 |
| 1.2 Research and development of Conformal Cooling Channels | 4 |
| 1.2.1 Development of design for conformal cooling channels .. | 5 |
| 1.2.2 Development of manufacturing for conformal cooling channels | 7 |
| 1.3 Overview of the research on the optimization design of conformal cooling channels | 11 |
| 1.4 Significance of the selected topic and the main research content | 14 |
| 2. ANALYSIS OF THE COOLING MECHANISM OF INJECTION MOLDS | 17 |
| 2.1 Injection mold cooling system | 18 |

| | |
|--|----|
| 2.1.1 The influence of cooling system on production efficiency | 19 |
| 2.1.2 The influence of cooling system on the quality of plastic parts | 21 |
| 2.2 Heat transfer analysis of injection molds | 23 |
| 2.2.1 Analysis of mold heat transfer system | 23 |
| 2.2.2 Analysis of heat transfer between plastic and mold | 25 |
| 2.2.3 Analysis of heat transfer between mold and coolant | 25 |
| 2.2.4 Analysis of heat exchange between mold and natural environment | 27 |
| 2.2.5 Analysis of heat transfer between mold and injection molding machine table | 28 |
| 3. MATHEMATICAL MODELING OF HEAT TRANSFER WITH CONFORMAL COOLING CHANNELS | 30 |
| 3.1 Model assumptions | 30 |
| 3.2 Model establishment | 31 |
| 3.2.1 Thermal conductivity model inside the product | 31 |
| 3.2.2 Cooling channels convective heat transfer model | 33 |
| 3.2.3 Heat transfer model of the mold | 36 |
| 4 DESIGN ANALYSIS OF CONFORMAL COOLING CHANNELS | 39 |
| 4.1 The general principles of cooling channels design | 40 |
| 4.2 Simulation analysis of cooling channels with different | |

| | |
|---|-----------|
| configurations | 42 |
| 4.2.1 Introduction to one-way analysis of variance | 42 |
| 4.2.2 The influence of the cross-sectional shape of cooling channels on cooling effectiveness | 45 |
| 4.2.3 The effect of the type of cooling channel arrangement on the cooling effect | 50 |
| 5 MULTI-OBJECTIVE OPTIMIZATION OF THE DESIGN FOR CONFORMAL COOLING CHANNELS | 56 |
| 5.1 Introduction to experimental optimization | 57 |
| 5.1.1 Orthogonal experiments | 57 |
| 5.1.2 Response surface methodology | 59 |
| 5.1.3 Genetic algorithm for multi-objective optimization | 60 |
| 5.2 Screening of optimization variables | 63 |
| 5.3 Optimal experimental design and analysis of results | 66 |
| 5.3.1 Determination of optimization variables and response indicators | 66 |
| 5.3.2 Response Surface Design of Experiments | 69 |
| 5.4 Multi-objective optimization | 82 |
| 6 DESIGN SPECIFICATIONS AND EXAMPLE VERIFICATION OF CONFORMAL COOLING CHANNELS | 86 |
| 6.1 Design specifications for conformal cooling channels | 86 |
| 6.2 Cooling system design and cooling simulation based on UG and | |

| | |
|---|-----|
| Moldflow | 90 |
| 6.2.1 Establishment of finite element model | 90 |
| 6.2.2 Moldflow cooling analysis type selection | 91 |
| 6.2.3 Selecting the proper type of conformal cooling channels for thin wall products | 93 |
| 6.3 The design of conformal cooling channels for the products | 94 |
| 6.4 The model of the mold with conventional cooling channels | 95 |
| 6.5 Cooling channel design and modeling | 97 |
| 6.6 Analysis and comparison of cooling results | 98 |
| 7 SUMMARY AND CONCLUSIONS | 103 |
| REFERENCES | 104 |

LIST OF FIGURES

| | |
|---|----|
| Figure 1 Schematic diagram of conventional and conformal cooling channels | 7 |
| Figure 2 Injection mold cooling system | 18 |
| Figure 3 Cycle Time in injection molding | 20 |
| Figure 4 Typical mold temperature variation curve | 21 |
| Figure 5 Schematic diagram of mold temperature distribution | 25 |
| Figure 6 The heat transfer behavior of molten material during flow..... | 32 |
| Figure 7 Schematic diagram of thermal equilibrium of a cooling channel element with length dx | 35 |
| Figure 8 Schematic diagram of cooling channel layout..... | 42 |
| Figure 9 Plastic part structure | 47 |
| Figure 10 The model of cooling channels with different cross-section shapes..... | 48 |
| Figure 11 Temperature distribution of products at the end of cooling..... | 49 |
| Figure 12 Layout type of cooling channels | 51 |
| Figure 13 Plastic part B structure | 52 |
| Figure 14 Cooling channel models with different layout | 52 |
| Figure 15 Temperature distribution of products at the end of cooling | |

| | |
|---|-----|
| | 52 |
| Figure 16 NAGA-II procedure flowchart..... | 62 |
| Figure 17 Pareto optimal solutions set of 500 generations of evolution..... | 61 |
| Figure 18 Design of connection part of cooling channel..... | 88 |
| Figure 19 Model of plastic part and measurement of the wall thickness..... | 90 |
| Figure 20 Procedure of the analysis and simulation of the part by Moldflow..... | 91 |
| Figure 21 The model of the mold with simple spiral cooling channels..... | 93 |
| Figure 22 Local layout of the conformal cooling channel..... | 94 |
| Figure 23 The model of the mold with conventional cooling channels..... | 95 |
| Figure 24 Simulation results for the temperature of part after the cooling process..... | 99 |
| Figure 25 Detailed temperature distribution within the part..... | 100 |
| Figure 26 Time to reach ejection temperature of part..... | 102 |
| Figure 27 Distinct time for various sections of the part to reach the ejection temperature..... | 101 |

LIST OF TABLE

| | |
|--|----|
| Table 1 Injection molding process parameters | 46 |
| Table 2 Simulation Results of different cross-sectional shape | 48 |
| Table 3 Cooling time | 48 |
| Table 4 Uniformity of mold temperature distribution | 49 |
| Table 5 Variance analysis table (cooling time) | 49 |
| Table 6 Variance analysis table (mold temperature distribution uniformity) | 49 |
| Table 7 Simulation results | 53 |
| Table 8 Cooling time of parts with different cross-sections of cooling channels | 53 |
| Table 9 Uniformity of mold temperature distribution | 53 |
| Table 10 Variance analysis table (cooling time) | 53 |
| Table 11 Variance analysis table (uniformity of mold temperature distribution) | 54 |
| Table 12 Significant differences among different levels | 54 |
| Table 13 The range of design variables for different wall thicknesses of channels | 63 |
| Table 14 Orthogonal test plan and results | 64 |
| Table 15 Analysis of variance table | 64 |
| Table 16 Test result range analysis table | 65 |

| | |
|---|----|
| Table 17 Value ranges of cooling channel design variables with different wall thicknesses | 68 |
| Table 18 DOE-1, DOE-2, DOE-3 optimization specification | 68 |
| Table 19 DOE-1 DOE-2 DOE-3 values | 69 |
| Table 20 Box-Behnken Experimental Design Table | 70 |
| Table 21 DOE-1, DOE-2, DOE-3 test plan | 70 |
| Table 22 DOE-1, DOE-2, DOE-3 test result | 71 |
| Table 23 DOE-1 ANOVA Table (cooling time) | 73 |
| Table 24 DOE-1 ANOVA table (uniformity of part temperature distribution) | 73 |
| Table 25 DOE-2 ANOVA table (cooling time) | 76 |
| Table 26 DOE-2 ANOVA table (uniformity of part temperature distribution) | 76 |
| Table 27 DOE-3 ANOVA table (cooling time) | 78 |
| Table 28 DOE-3 ANOVA table (uniformity of part temperature distribution) | 79 |
| Table 29 The optimal solution and optimal result after evolution ... | 85 |
| Table 30 Optimization results and simulation results | 85 |
| Table 31 Design parameters of conformal cooling channel for curved shell products under ideal arrangement | 89 |
| Table 32 Injection molding process parameter setting | 97 |

ABBREVIATIONS

| | |
|---------|--|
| AM | Additive Manufacturing |
| BBD | Box-Behnken Design |
| CCD | Central Composite Design |
| DMLSR | Direct Metal Laser Sintering |
| EBM | Electron Beam Melting |
| FEM | Finite Element Methods |
| FDM | Fused Deposition Molding |
| LOM | Laminated Object Manufacturing |
| NSGA-II | Non-dominated Sorting Genetic Algorithm II |
| PLM | Plastic Injection Molding |
| RSM | Response surface methodology |
| SLM | Selective Laser Melting |
| SLS | Selective Laser Sintering |
| SFF | Solid Freedom Fabrication |
| SLA | Stereo Lithography Apparatus |

INTRODUCTION

1.1 Research background

With the rapid development of the economy, in the modern industrial system, the plastics industry has become a basic materials industry alongside with steel, cement and wood, and its industry has a wide consumer market and occupies an extremely important position in the world today. Compared with metal, stone, wood and other products, plastic products are light, low cost, plasticity, can be widely used in home appliances, automobiles, packaging, machinery, agriculture, medical, aerospace, and daily life, and other fields. Plastic products are so widely used, and their corresponding means of molding and processing are numerous. Common plastic molding and processing methods include injection molding, extrusion, calendaring, blister molding, blow molding, molding, and thermoforming, among which injection molding is the leading industry in the plastic processing industry. According to statistics, the cumulative value of plastic products output reached 71.995 million tons, of which the output of injection molding products accounted for about 38% of the total output of the plastic products industry in the same period, and most plastic products in daily life are molded by injection molding process.

The injection molding process is divided into 5 stages, namely mold closing, injection, pressure holding, cooling, and demolding, all of which rely on the mold[1]. [4] Among them, injection and cooling stages have a decisive influence on the molding quality of products, and the cooling stage is the most important, accounting for about 70% ~ 80% of the whole injection molding cycle, which directly determines the production efficiency of injection molding. Therefore, in the injection molding

process, under the premise of ensuring product quality, the time of each stage of the molding cycle should be shortened as much as possible, especially the cooling stage. This then requires the design of an efficient mold cooling system that can significantly improve the cost effectiveness and molding quality of injection molding.

With the increasing improvement of people's living standard and the rise and development of new manufacturing industries such as new energy vehicles, medical devices, intelligent manufacturing and Industry 4.0 in China, the domestic injection molding products market, especially the high-end injection molding products market, has been further stimulated by the demand for high-precision, high-quality and high-complexity products. To meet the market demand, more and more products are designed into complex and delicate shapes to attract consumers' attention, and they contain various complex curved structures, which increasingly put forward higher demands on the cooling technology of injection molds.

Traditional mold cooling technology is difficult to meet the production needs of today's high-end complex products, because the traditional cooling channels is mostly drilled in a straight line, and the distance from the channels to the cavity varies so that the mold is difficult to obtain uniform temperature distribution, which makes the cooling shrinkage of plastic parts inconsistent, resulting in the existence of residual stress, causing the product to warp deformation or cracking, etc.; furthermore, for large complex cavities of the mold, the longtime uneven mold temperature distribution will cause differences in thermal deformation of various parts of the cavity, affecting the mold fit accuracy and product dimensional stability. In addition, for large and complex cavity molds, the longtime uneven temperature distribution of the mold will make the thermal deformation of various parts of the cavity differ, which affects the

precision of the mold and the dimensional stability of the product. Secondly, the distance between the cooling channels and the cavity is different, which makes the cooling rate of different parts of the plastic part different. Therefore, it is very important to design an efficient cooling system to improve the molding quality and productivity of the molded parts for injection molding production.

In recent years, with the rapid development of metal 3D printing technology, the high-end process of mold technology has been advanced, and has made significant reforms and breakthroughs. The use of metal 3D printing manufacturing with the shape of the cooling mold effectively improves production efficiency, shortens the production cycle, and improves the molding quality of products, bringing good economic benefits to enterprises. Nowadays, many studies have been carried out at home and abroad on the conformal cooling channels, which has proved the high efficiency of the conformal cooling channels, but the engineering practice has proved that the cooling efficiency and cooling uniformity of the conformal cooling channels have not fully met the needs of high-end products, and the conformal cooling system still needs to be optimized.

Due to the limitations of mold manufacturing technology, previous optimization was generally limited to the traditional straight-drill type channels, using devices such as water separators, bubblers or hot pins to improve cooling in small localized areas away from the main cooling channels to achieve improved cooling efficiency and cooling uniformity.

Nowadays, with the increasing maturity of metal 3D printing technology, the conformal cooling system has been widely used. How to optimize the design of the conformal cooling channels to maximize its value has gradually become the focus of research in this field and has become a frontier topic for research in the world.

1.2 Research and development of Conformal Cooling Channels

Conformal Cooling Channel (CCC) is a cooling water channel that changes with the shape of the product contour, as shown in Fig. 1. Compared with the traditional cooling water channel, Conformal Cooling Channel is no longer linear, which can solve the problem of inconsistent distance between the traditional cooling water channel and the surface of the cavity, make the temperature of the mold cavity evenly distributed, achieve efficient and uniform cooling of injection molded products, eliminate warpage and deformation and other defects, shorten the manufacturing cycle of plastic products, improve production efficiency, enhance the competitiveness of enterprises, and has strong

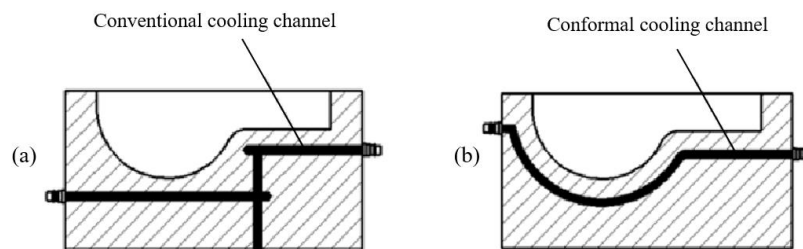


Figure 1 Schematic diagram of conventional and conformal cooling channels
applicability.

As early as 1997, Professor E. Sachs of MIT proposed and researched injection mold conformal cooling technology, which he believed would become one of the four most important applications for 3D printing. With the development of shape cooling technology, the development of complex mold cooling technology has also been promoted. In recent years, domestic and foreign research has been carried out on injection mold shape-based cooling channels, and certain achievements have been made.

1.2.1 Development of design for conformal cooling channels

In the design of the injection mold with the shape of the cooling channels, the design method, layout, and spatial structure of the cooling channels has been carried out numerous studies.

In 2000, Xu et al. of MIT first proposed six design rules for injection mold with-shape cooling channels: design of with-shape cooling conditions, design of cooling medium pressure drop, design of cooling medium temperature uniformity, design of adequate cooling, design of uniform cooling and design of mold strength. This design guideline provides some theoretical guidance for the design of the water channel with the shape, but the cooling unit proposed by this design guideline is only a two-dimensional unit with low precision, and there is a certain gap between it and the actual effect.

In 2001, Li et al. of the City University of Hong Kong proposed a model-based feature identification algorithm for the design of conformal cooling channels layout. It decomposes a complex-shaped plastic part into several simple features and designs each feature separately according to the heat transfer properties of plastic and mold as well as the divided plastic part features, and then combines the cooling channels of all feature units to form the cooling system of the whole injection molded product. The feasibility of this design method was verified by analyzing the design example of this method using C-MOLD software. The disadvantage is that the feature recognition algorithm also has the limitation of geometry coverage, which is not applicable to all complex parts, and the method does not consider the difficulty of cooling channels processing. To solve the problem of machining feasibility, Li et al. improved the feature-based algorithm and again proposed the design idea of conformal cooling channels based on the "path search algorithm" in 2004, which generates

the schematic diagram of the conformal cooling channels.

In 2005, Fred et al. of D-M-E proposed a porous shaped cooling structure based on the coal mine model, which has a larger specific surface area for heat exchange and higher heat transfer efficiency, and the cooling efficiency can be increased by more than 40 % compared with the traditional linear cooling channels.

In 2007, Zhigang Wu and Yusheng Shi from Huazhong University of Science and Technology in China proposed a design method for the conformal cooling channels based on the discrete/aggregate model based on the transient heat transfer process and the processability problem and manufactured a soap box mold with conformal channels for example verification, and the experiment showed that the cooling effect was significantly improved.

In 2007, Au et al. proposed a scaffold-shaped water channel structure. The scaffolded cooling system with a porous structure was formed by using spatial enumeration to assemble one scaffold unit divided by a mold. In 2009, Wang et al. proposed conformal cooling channels with a discrete center-of-mass (CVD) van Nogram mesh structure. Both Au and Wang's proposed cooling channels have large heat transfer area and can cool the molded part quickly and uniformly, but the cooling channel structure is complicated, and the local size is too narrow and easy to be blocked.

In 2013, Alban et al. in France designed conformal cooling channels by solving the melt temperature distribution on the cavity surface using a conjugate algorithm and Lagrange method with product quality and production efficiency as the objective functions, but the performance of the cooling channels was not optimal. In the same year, Jauregui-Becker et al. developed an automated design software for the with-shape cooling channels, however, the method was limited to the design of with-shape

cooling channels for low-complexity, simple cross-section parts due to the diversity of product shapes and the variability of cooling schemes.

In 2018, Marin et al. of the Federal University of Santa Catarina, Brazil, proposed a new shaped cooling channels with a combination of series and parallel modes. This cooling method has a larger cooling area and parallel coolant inlet and outlet, which can achieve better temperature homogenization, but there are also problems that are not easy to process.

1.2.2 Development of manufacturing for conformal cooling channels

Despite the incomparable advantages of the traditional cooling technology, it is difficult to manufacture the follower cooling channels using the traditional mold processing method, which to a certain extent limits the application of the follower cooling technology. For this reason, domestic and foreign research scholars and mold companies have carried out in-depth exploration of the manufacturing of the conformal cooling channels, from the early casting of copper channel bending indirect mold making and milling-based traditional machining mold making, to the use of cutting-edge metal 3D printing technology mold making, multiple solutions to the manufacturing of the conformal cooling channels, promoting the development of the conformal cooling technology.

In 1998, Jacobs in the UK used a conventional mold turning technique to bend and fix copper tubes in a prefabricated electroformed nickel shell mold and cast copper as a filler material to form a conformal cooling mold. The study showed that the parts produced by this mold had more uniform heat distribution and good surface finish. He Yin from Hubei University of Technology in China used graphite as the substrate material, combined with plasma deposition process, and used copper channel bending to manufacture injection molds with conformal cooling channels, and the cooling effect of the mold was substantially improved compared

with the traditional linear channels.

However, there are many shortcomings, as the copper tube can only partially follow the shape, and when the part is too complex with depressions or bumps, the copper tube cannot provide good followability, and the interface with the filling substrate also affects the heat transfer. Therefore, some researchers are also exploring the use of traditional machining methods to create conformal cooling channels to overcome these difficulties.

In 2004, Sun et al. proposed a U-shaped milling groove with conformal cooling channels based on traditional machining means for large and complex parts, especially those with large free-form surfaces. Sun used the finite element analysis software Abaqus to simulate and compare the cooling effect of U-shaped milling groove and linear drilling channels, and found that the U-shaped milling groove with shaped channels has better temperature distribution and cooling time than linear drilling channels. better temperature distribution and cooling time.

Around 2010, Park and Dang of the University of Ulsan, Korea, fabricated injection molds with [9] conformal cooling channels using conventional machining methods. Park used a drilling technique to produce an array of spacer plates close to the surface of the mold cavity for conformal cooling, and Dang used a milling technique to produce a U-shaped cross-sectional mold for conformal cooling. Both are relatively simple to process, and the cooling effect is significantly better than the traditional cooling channels, but there is a problem of possible coolant leakage.

In 2016, Rahim et al. in Malaysia used machining to fabricate new milled slotted square follower-shaped cooling channels with larger effective cooling area than circular cross-section and other types of cooling channels.

With conventional machining methods, the fabrication of cooling channels is certainly simple, but they are highly susceptible to cooling water leakage problems, and milling-type machining usually requires the mold to be assembled in a panel, which has an impact on the strength and life of the mold.

With the development of metal 3D printing technology, conformal cooling channels have been applied to the cooling of complex injection molded products. 3D printing technology can complete the manufacturing of complex processes that cannot be produced by traditional manufacturing processes, which is a good solution to the problem of traditional processing means cannot produce complex shaped cooling channels and shorten the manufacturing cycle.

Metal 3D printing technology is also known as Additive Manufacturing (AM), which is an additive manufacturing technology that uses materials to accumulate layer by layer. The product is modeled by computer, the 3D model of the product is sliced and processed using control software, and the raw materials are stacked layer by layer by a 3D printer to make the 3D data model into a 3D solid. Common 3D printing technologies include Direct Metal Laser Sintering (DMLS), Selective Laser Sintering (SLS), Light Curing Stereo Lithography Apparatus (SLA), and Selective Laser Fusion. SLA), Selective Laser Melting (SLM), Direct Metal Laser Sintering (DMLS), Laminated Object Manufacturing (LOM), Electron Beam Melting (EBM) (LOM), Electron Beam Melting (EBM), Fused Deposition Modeling (FDM), and Three-Dimensional Printing (3DP), etc.

As early as 2000, Sachs et al. used 3DP technology to create a mold with a highly complex internal geometry with conformal cooling channels and found that the cooling time of the resulting product was reduced by 15% and the warpage was reduced by 9%, resulting in a more accurate control of the molding temperature and a reduction in the

residual stress of the part. In 2007, Ranner et al. at the University of Sweden studied the use of EBM technology to make a conformal cooling injection mold and investigated the warpage deformation of the molded part by using the conformal cooling channels and the traditional linear cooling channels.

Huazhong University of Science and Technology has conducted a more in-depth study on the fabrication of channels molds with shape. Lu Zhongliang et al. and Shi Yusheng et al. used the SLS technology to fabricate a carbon steel alloy battery box with conformal cooling injection mold and a soap box with conformal cooling mold, respectively. Liu Bin et al. used SLM to fabricate a conformal cooling injection mold for a machine tool cooling water pump impeller and obtained a mold insert with a conformal cooling channel. In 2016, the Center for Additive Manufacturing of Huazhong University of Science and Technology integrated the design of conformal cooling channel, SLM with mold material and crack resistant SLM process technology to achieve rapid manufacturing of complex conformal cooling molds, and the strength, corrosion resistance and hardness of the optimized molds after SLM printing and molding exceeded the level of castings and were close to forgings. According to the production application, the cooling efficiency of the SLM-cooled molds is 50% higher than that of traditional molds, and the deformation of the parts is significantly reduced.

The emergence of metal 3D printing technology, free from the traditional processing methods of many restrictions on the water processing, so that the water layout closer to the product contour. At the same time, for the general product dead ends or areas not easy to dissipate heat, such as localized bumps or depressions, with the conformal cooling channels can provide good cooling efficiency, and therefore has traditional cooling channels cannot be compared to the cooling effect. In

recent years, the industry is exploring the combination of 3D metal printing and traditional mold manufacturing technology and optimize the design of the channels to improve the cooling efficiency and molding quality of complex molds, thus promoting the high-level development of mold cooling technology.

1.3 Overview of the research on the optimization design of conformal cooling channels

The design of injection molding cooling system will directly affect the quality and cooling efficiency of products. An effective cooling channel system can provide uniform temperature distribution in the mold cavity, reduce warpage and deformation of the molded part, reduce cooling time, and improve the quality of the molded part. For the research of the following cooling water channel, domestic and foreign have proved the efficiency of the cooling technology, but the engineering practice proves that the cooling efficiency and cooling uniformity of the following cooling water channel cannot fully meet the needs of high-end products, the following cooling water channel still needs to be optimized. Therefore, the optimization of the design of the conformal cooling channels becomes an important research content.

Based on different optimization methods, the variable parameters of cooling channels optimization design mainly include the arrangement of cooling channels, cross-section size, cross-section geometry, as well as the distance between adjacent channels and the distance from the center line of channels to the cavity, etc. The objective function of optimization mainly includes the uniformity of mold temperature distribution and cooling time, etc.

Most of the optimization for the conformal cooling channels is based on the parametric tasks of finite element, generally using experimental

design or optimization algorithm to optimize the design parameters of the cooling channels, to get the best design of the following shaped cooling channels.

Saifullah (Australia) and Dimla (UK) have optimized the design of the cooling channels by finite element simulation analysis, in which Dimla et al. used I-DEASTM software to determine the optimal design of the cooling channels of the injection mold by establishing a CAD model of the product and finite element thermal analysis of the core and cavity. Saifullah et al. used Pro-Engineer software to develop a circular-shaped cooling channel with a cross-section and optimized the design of the cooling channels of the plastic bowl injection mold with the cooling time as the optimization target and analyzed the optimized cooling water channel with the help of ANSYS simulation software. The optimized cooling water channel was analyzed with the help of ANSYS simulation software, and it was found that with proper geometric cross-section and layout design, the cooling time could be shortened by 40% and the molding cycle by 35%, thus greatly improving the production efficiency and product quality.

Jahan, USA, and Venkatesh, India, investigated the optimal design parameters of the conformal cooling channels using a design-of-experiment approach. The effect of the critical design parameters on the thermal performance of the mold was investigated by Jahan et al. The study took a plastic part with a wall thickness of 1.5 mm as an example. Through the experimental design of three parameters, the diameter D of the mold cavity with shaped cooling channels, the distance P of the adjacent channels, and the distance L from the center line of the channels to the cavity, the optimal cooling effect was obtained when $D=6$ mm, $P=8$ mm and $L=4$ mm, and the cooling time was shortened to 12.76s.

Choi et al. from Korea proposed an automated design optimization method for the cooling channels with shape. Taking eyeglass lenses as an example, they optimized the design of the conformal cooling channels by simulating the growth mechanism of plant roots with the optimization goal of minimizing the deviation of the product surface temperature. The method first uses the CVD algorithm to divide the product into smaller areas, then uses the binary branching law to connect the thermal centers to form cooling channels and evolves through channel branching until the channels reach the minimum diameter or the maximum allowable pressure drop. It is shown that the temperature deviation of the product can be reduced by about 30% using the evolutionary optimization method, which is good for improving the mold temperature uniformity and reducing the volume shrinkage.

Venkatesh et al. evaluated the thermal performance of a single-cavity injection mold by ANSYS using a similar method with mold temperature uniformity and cooling time as the optimization objectives, and used Taguchi's method to orthogonally design three parameters of the cooling channel cross-section shape, path arrangement form and distance between the adjacent channels to optimize the design of the follower cooling channel, and found that the follower cooling channel with a spiral circular cross-section. It was found that the spiral circular cross-sectional cooling channel has better cooling temperature distribution. Compared with Jahan's optimization, Venkatesh's design overcomes the shortcomings of single-objective optimization and achieves multi-objective optimization of mold temperature uniformity and cooling time, which has better applicability.

Based on COMSOL software simulation, Wu et al. in the United States carried out parameter optimization based on thermodynamic finite element model and multi-scale thermodynamic topology optimization,

and obtained the optimal design parameters of the cooling channel by using derivative-free optimization solution, and optimized the distribution of the cell lattice by solving the thermodynamic topology optimization problem to form a multiphase lattice structure, which makes the mold lightweight and ensures the structural strength of the mold. Compared with other optimized designs, this optimized design improves the structural stability of the injection mold while ensuring the optimal water channel design.

Shi Yusheng, China, used finite element simulation method to optimize the best cooling channel for the incense box parts by simulating and analyzing two different shaped cooling schemes with the help of Moldflow software. The simulation results show that the cooling effect of the circular structure cooling channels is better than that of the spiral cooling structure, and its productivity is increased by 30% compared with the conventional mold, and the warpage deformation is only 20% of that of the common mold.

1.4 Significance of the selected topic and the main research content

The production efficiency of injection molding and the quality of the products directly affect the economic efficiency of enterprises. As the demand for curved products, especially high quality complex curved products, increases, it is important to improve the surface quality and production efficiency of these products. Based on this situation, the further research of injection molding cooling technology with shape is very critical.

From the above research progress, the research of the with-shape cooling technology mainly focuses on the design and manufacturing of

the with-shape channels, in terms of the design rules of the with-shape channels, the structural design of the channels and the mold manufacturing. For the optimization design of the conformal cooling channels, certain research results have been achieved at home and abroad, and several optimization design methods have been established to promote the development of the optimization technology of the cooling conformal cooling channels. However, most of the optimization is limited to the theoretical stage of mold flow simulation, with little practical verification, and the efficiency of the existing multi-objective optimization methods is low. Based on this status quo, this paper optimizes the design of the conformal cooling channels by optimizing the experimental design and optimization algorithm and solves the optimal design parameters for products with different wall thicknesses, so as to propose the design specification of the conformal cooling channels to guide the mold design and promote the improvement of the production efficiency of enterprises.

This paper will be based on the following aspects of research:

(1) Theoretical research on cooling of injection molds. Thermodynamic analysis of the process and mechanism of heat transfer in the mold during injection molding, the establishment of a mathematical model of heat transfer in the conformal cooling channels, and the investigation of the factors affecting the cooling effect.

(2) Design variable significance examination. The single-factor test method was used to study some of the design variables of the conformal cooling channels to examine whether they have significant effects on the cooling effect.

(3) Optimization of the design variables of the conformal cooling channels. Firstly, the orthogonal test method was used for factor screening to determine the design variables affecting the cooling channels.

Then, the multi-objective optimization algorithm combining response surface method and NSGA-II is used to optimize the design of injection molding with shaped cooling channels for products of different thicknesses with the cooling time and cavity temperature uniformity as the optimization objectives, and the Pareto optimal frontier solution set of the optimization objectives is obtained to obtain the best design parameters, to propose a perfect optimization design specification.

(4) Verification of typical product examples. Based on the proposed design specification, the optimized design of the water channel is carried out for a typical product example, and the practicality and reliability of the optimization results are investigated through Moldflow simulation to verify whether the proposed design specification can significantly improve the cooling effect of the product.

2. ANALYSIS OF THE COOLING MECHANISM OF INJECTION MOLDS

The cooling phase of injection molding is a complex process involving thermodynamics and fluid mechanics, which directly affects the molding quality and productivity of the molded parts.

2.1 Injection mold cooling system

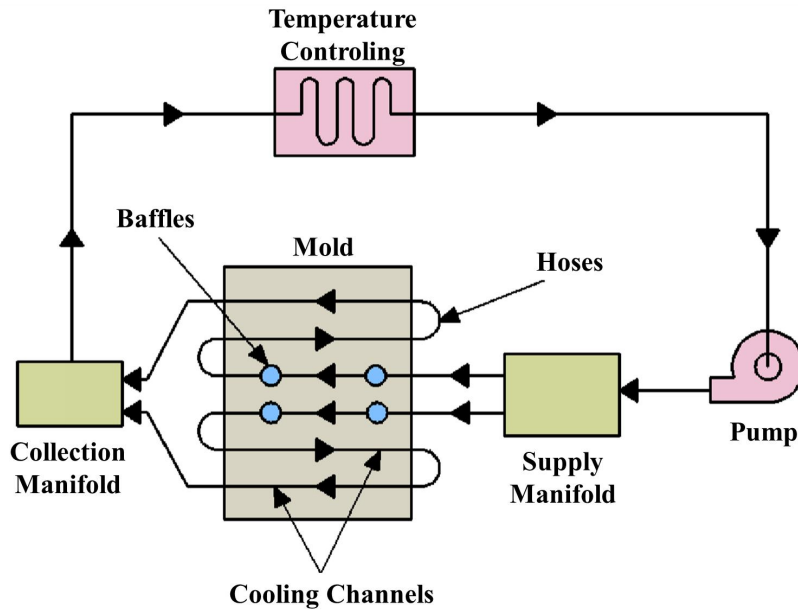


Figure 2 Injection mold cooling system

A common injection mold consists of several parts such as pouring system, cooling system, molding parts, guiding mechanism, and demolding mechanism. Among them, the injection mold cooling system, also known as mold temperature control system, is a device to heat or cool the mold, which usually consists of mold temperature machine, water pump, coolant supplier, cooling channels, hose and coolant collector, as shown in Fig. 2.

In actual production, the mold temperature is usually regulated through the circulation of heat transfer or cooling medium in the cooling water channel, to achieve the purpose of raising or lowering. Common heat transfer or cooling medium using water and oil, where oil is used for higher working temperature than water coolant, usually operating between 100°C and 350°C, and because the specific heat of water than oil, heat transfer coefficient is large, low cost, so the general production is usually water as a cooling medium for temperature control. And to make

the plastic parts cool quickly, the coolant must be carried out using turbulent flow state, thus increasing the heat transfer area. In the whole production cycle of the mold, the coolant will be delivered throughout the injection molding stage, except for the mold closing and opening process, the coolant will continue to effectively cool the mold. Depending on the product and the mold, the cooling system will be designed differently and will exhibit different cooling efficiencies.

2.1.1 The influence of cooling system on production efficiency

After the resin is heated and melted, driven by the injection molding machine screw or piston, it is injected into the mold cavity through the injection molding machine nozzle through the mold casting system, then cooled and cured and ejected from the mold in a series of actions that is the injection molding process. This process can be roughly divided into five stages: mold closing, injection, pressure-holding, cooling and demolding, which form the whole cycle of injection molding. In injection molding production, from the first time the mold is closed to inject plastic melt to the time when the mold can reach a stable production state, there will be several cycles of adaptation period, that is, the trial production period, which also has a great impact on the production efficiency. Therefore, the impact of the cooling system on productivity can be summarized in two aspects: the impact on the molding cycle and the impact on the trial production period.

- (1) The cooling system's influence on the molding cycle

The time distribution of each stage in a typical injection molding cycle is shown in Fig. 3. Obviously, reducing the cooling time in the molding cycle is the key to improving productivity, and the cooling time depends on whether the cooling system is efficient.

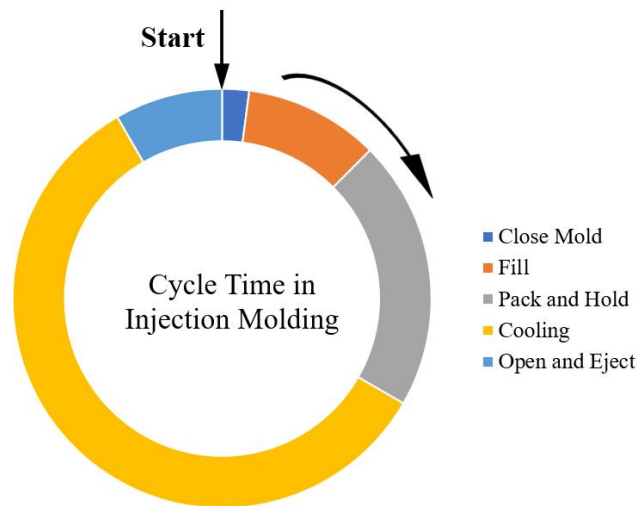


Figure 3 Cycle Time in injection molding

(2) The cooling system's influence on the trial production period

When the mold is produced, the mold usually has a certain temperature to ensure the quality of the product molding. For large molds, because each injection of trial production period is also accompanied by the process of cooling, the accumulation of heat is gradual, and the trial production period may be if several hours immediately after the cooling of the products, which greatly increases the production cost of enterprises, so the mold temperature is usually raised to the set temperature by preheating. However, for most molds, it is usually through the heat accumulation of the products during the trial period to reach the suitable or set temperature, as shown in Fig. 3. It is the mold temperature change process curve when the mold reaches the stable state. Therefore, to ensure faster attainment of a stable state for the mold, it is crucial to design a highly efficient cooling system that rapidly removes the accumulated

heat.

2.1.2 The influence of cooling system on the quality of plastic parts

During the production of plastic parts, the cooling system of injection mold controls the change of mold temperature, and the level and distribution of mold temperature has a great influence on the quality of products.

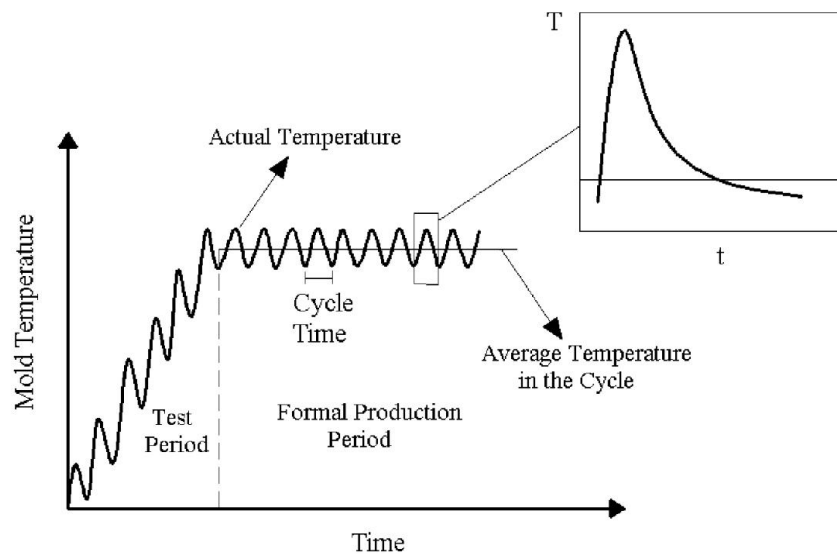


Figure 4 Typical mold temperature variation curve

(1) The influence of mold temperature on the quality of products

The temperature of the mold directly affects the flow state and crystallization behavior of the plastic melt. For amorphous plastics, the mold temperature mainly affects the viscosity of the plastic melt when filling the mold. If the mold temperature is too low, the melt viscosity will be large, which will lead to stagnation and defects such as short shot and fusion marks, and the low mold temperature will lead to dent and internal stress due to fast cooling rate. Shrinkage rate, also easy to lead to product ejection deformation problems.

For crystalline or semi-crystalline plastics, the mold temperature directly affects the crystallinity of the plastic product. The physical and

chemical properties of crystalline polymer products are related to the crystallinity, crystalline form, and crystal morphology of their polymers, and most of these structures are also dependent on the mold temperature. If the mold temperature is too low, the crystallization temperature interval is short, which is not conducive to the crystallization behavior and is not good for maintaining the dimensional stability of the plastic part, but reduces the shrinkage of the plastic part; if the mold temperature is too high, the crystallinity of the plastic part will increase and the mechanical properties (such as hardness, tensile strength, etc.) and dimensional stability of the product will be improved, but if the crystallinity is too high, the plastic part will be easy to crack. Therefore, in the actual production, it is necessary to balance the various effects and regulate the reasonable mold temperature to ensure the best molding effect.

(2) The influence of mold temperature distribution on the quality of products

The distribution of mold temperature directly affects the surface quality and physical and mechanical properties of the products. If the cooling system is not designed properly, it will lead to uneven temperature distribution of the mold, and the degree of shrinkage of each part of the product will be different, thus forming the internal stress of the plastic parts, affecting the physical and mechanical properties of the products, resulting in the decrease of the mechanical strength of the products; at the same time, uneven cooling is also prone to warpage and deformation, especially for the plastic parts with uneven wall thickness and complex shape, which will affect their shape and dimensional accuracy, so the design of the cooling system is particularly important. Therefore, the design of the cooling system is particularly important.

Therefore, the control of mold temperature in the injection molding process is one of the cores of the injection molding process, so the design

of the injection mold cooling system is also the focus of the injection mold design, which has a direct and significant impact on the molding quality and production efficiency of the products.

2.2 Heat transfer analysis of injection molds

A series of heat exchange occurs after the plastic melt enters the cavity of the mold. Therefore, when studying the water-cooling problem of injection molding, we must first understand the thermal behavior in the mold physically and mathematically, and understand how the products transfer heat to the mold, and how the mold transfers heat to the cooling medium or other objects, which requires us to master the mechanism of heat exchange. Before an injection mold can work stably, produce qualified products, and enter into production period, it needs to go through several cycles of adaptation period, i.e., trial production period. After the trial period, the mold will reach a stable state with a constant average temperature. This section only analyzes the heat transfer after the mold reaches the steady state.

2.2.1 Analysis of mold heat transfer system

To facilitate analysis, heat transfer is divided into three ways in heat transfer according to the heat transfer mechanism: heat conduction, convection, and thermal radiation. Heat conduction refers to the process of heat transfer from high temperature region to low temperature region in the medium (solid, liquid or gas) or when different mediums are in direct contact, which has no relative motion of macroscopic objects, only thermal motion of microscopic particles. Convection is the heat transfer between the solid and the flow, and this process has the macroscopic motion of the fluid. And thermal radiation is the electromagnetic wave emitted to the surrounding medium due to the thermal motion of microscopic masses within the object, which can be achieved without

direct contact between objects.

In plastic molding, the mold can be considered as a heat exchanger. Most of the heat brought in by the high temperature melt is transferred to the mold in contact with it, and then transferred by the mold to the coolant, the external environment, or the table in contact with the mold through different transfer methods, thereby completing the cooling of the product. During the production cycle, the heat loss brought into the cavity by the plastic melt of the mold can be divided into three parts: (1) the heat carried away by the coolant; (2) the heat emitted from the outer wall of the mold to the natural environment; (3) the heat transferred from the mold to the table of the injection molding machine.

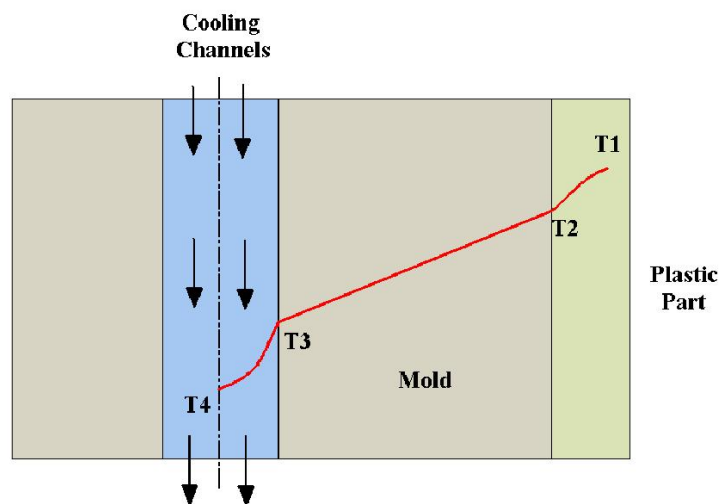


Figure 5 Schematic diagram of mold temperature distribution

The direction of the arrow indicates the heat transfer direction, and the annotation on the arrow shows the heat transfer method. Fig. 5 shows a typical mold temperature distribution diagram, with the heat dissipation, the mold temperature decreases sequentially from the plastic part to the channels mold.

According to the law of conservation of energy, combined with the above analysis, the heat balance equation of the mold in a stable production state during the injection molding process is obtained as

follows:

$$Q_P = Q_M = Q_C + Q_N + Q_E \quad (2-1)$$

where Q_P is the heat released by the plastic melt, Q_M is the heat transferred from the plastic melt to the mold, Q_C is the heat carried away by the coolant, Q_N is the heat emitted from the outer wall of the mold to the natural environment, Q_E is the heat transferred from the mold to the injection molding machine workbench.

2.2.2 Analysis of heat transfer between plastic and mold

As the plastic melt is injected into the mold cavity, heat is carried into the mold, and then the cooling melt is cooled. In this process, the plastic and the mold conduct heat through the surface of the cavity. Assuming that all the heat released from the plastic is transferred to the mold, and then transferred from the mold to the coolant and the external environment, the heat released from the cooling of the plastic part to the end of the cycle is

$$Q_M = Q_p = c_p \rho_p V (T_M - T_E) + \varphi \quad (2-2)$$

where c_p is the specific heat capacity of the plastic, ρ_p is the density of the plastic product; V is volume of the cavity; T_M is the temperature of the melt injected into the cavity; T_E is the temperature of the product at the end of cooling; φ is the latent heat of crystallization of the crystalline polymer.

2.2.3 Analysis of heat transfer between mold and coolant

Mold heat is first transferred from the wall of the channels to the coolant through heat conduction, which raises the temperature of the coolant, and then the heat is taken away through the movement of the coolant, followed by the contact of the coolant with the wall immediately afterwards to continue to take away the heat. Therefore, when the coolant flows along the water channel, the heat is transferred along the normal

direction of the wall of the cooling channels through the thermal conductivity of the coolant on one side, and the heat is taken away through the macroscopic displacement of the coolant on the other side. The convective heat exchange between the mold and the cooling medium is not only related to the thermal conductivity of the cooling medium, but also closely related to the movement of the cooling medium.

In production, for efficient heat exchange, the flow of coolant is driven by external forces (such as pumps), so the fluid in the channels is usually forced movement (forced convection) and turbulent state. The convective heat transfer is calculated as

$$Q_c = h_1 A_1 (T_W - T_C) \quad (2-3)$$

where h_1 is the convective heat transfer coefficient, A_1 is the convective heat transfer area of the channels, T_W is the average temperature of the cavity wall, T_C is the temperature of the coolant.

When the cooling channels is a circular channel, the water flow in the channel is turbulent, forced convection heat transfer in the channel, convection heat transfer coefficient h can be obtained by approximating the following formula

$$h = 2041 \times \frac{(1+0.015T_a)u^{0.87}}{D^{0.13}} \quad (2-4)$$

where T_a is the average temperature of the cooling water and D is the diameter of the cooling channels.

The heat transfer behavior between the mold and the coolant is influenced by the temperature at the coolant inlet, the convective heat transfer area and the convective heat transfer coefficient, which is actually a complex function of the flow rate U of the coolant fluid, the wall temperature T_W , the fluid temperature T_C , the fluid properties and the design parameters, geometry and location arrangement of the cooling channels. To improve the convective heat transfer capacity of the cooling

channels, it is necessary to increase the heat transfer area, which requires the optimal design of the cooling channels. At the same time, to strengthen the heat transfer, the water flow in the channel needs to be forced to move in a turbulent state. According to fluid mechanics, when the Reynolds number $Re > 4000$, the cooling medium in the channel will show a turbulent state, and in the actual injection molding production, the convective heat transfer coefficient will be in a more ideal value range when the Reynolds number $Re > 10000$ is in turbulent state.

2.2.4 Analysis of heat exchange between mold and natural environment

There are two ways of heat exchange between mold and natural environment: one is heat exchange by convection of air, because the movement of air is caused by the difference of density due to the difference of air temperature, so the convection method belongs to natural convection. The second is the radiation heat exchange caused by the contact between the outer wall of the mold and the air.

(1) Convective heat transfer

The convective heat exchange between mold and coolant has a more complete heat transfer analysis theory, and the convective heat exchange coefficient can be calculated more accurately. The convective heat transfer between the mold and the air is more based on empirical or experimental values because the influence of the air flow state must be considered. In normal production, in addition to the four sides of the mold exposed to the air, the dynamic and fixed mold surfaces where the parting is located when the mold is opened are also involved in convective heat transfer, so the heat transferred from the mold to the natural environment through convection is

$$Q_a = hA_2(T_m - T_a) \quad (2-5)$$

where,

$$A_2 = A_c + A_f \quad (2-6)$$

where, Q_a is the heat transferred from the mold to the natural environment; T_m is the average temperature of the surface of the mold; T_a is the air temperature of the surrounding environment; A_2 is the surface area of the mold for convective heat transfer; A_c is the area of the mold sidewall exposed to the air; A_f is the surface area of the movable and fixed mold where the mold is parted when the mold is opened.

(2) Radiation heat exchange

The heat transfer from the mold to the natural environment through thermal radiation is:

$$Q_f = A_m \varepsilon \sigma \left[\left(\frac{T_j + 273}{100} \right)^4 - \left(\frac{T_k + 273}{100} \right)^4 \right] \quad (2-7)$$

where, Q_f is the heat radiated into the air by the mold; σ is the Stephen Boltzmann constant; T_j is the average temperature of the surface of the mold; T_k is the ambient air temperature; ε is the blackness value. When the surface temperature of the polished steel plate is $-18 \sim 150^\circ\text{C}$, the value range of ε is $0.08 \sim 0.14$.

In summary, the heat emitted from the outer wall of the mold to the surrounded environment is

$$Q_N = Q_a + Q_f \quad (2-8)$$

2.2.5 Heat transfer between mold and injection molding machine table

The heat exchange between the mold and the injection molding machine table is carried out by heat conduction. When two solid substances are in direct contact, the contact thermal resistance exists

because the roughness of the solid surface often leads to unequal temperatures at the contact surfaces. Since the contact thermal resistance is much smaller compared with other thermal resistances and can be neglected, we assume that the mold is in close contact with the injection molding machine table without gap and the contact thermal resistance is zero, then the heat transfer from the mold to the injection molding machine table is

$$Q_E = h_2 A_3 (T_j - T_k) \quad (2-9)$$

where, A_3 is the contact area between the mold and the worktable of the injection molding machine; h_2 is the heat transfer coefficient between the mold and the worktable.

3. MATHEMATICAL MODELING OF HEAT TRANSFER FOR CONFORMAL COOLING CHANNELS

The conformal cooling channels manufactured by 3D printing have complex shapes. However, the commonly used circular cross-section cooling channel also has advantages. Its structure is simple and it is easy to control the flow state of the cooling liquid, and it can ensure the structural strength requirements of the mold. Therefore, it is necessary to analyze the heat transfer of the mold for the channel cooling water circuit. This chapter takes the circular section cooling waterway commonly used in engineering practice as the analysis object, establishes the mold heat transfer model, and analyzes the influencing factors of waterway heat transfer.

3.1 Model assumptions

Through the previous analysis, we know that the process of mold heat transfer involves three types of heat transfer: heat conduction, heat convection and heat radiation. They are heat conduction between the plastic melt and the mold, heat convection between the mold and the coolant, and convection and heat radiation between the mold and the natural environment, respectively. In actual production, the heat loss through the exterior of the mold facing the natural environment is less than 5%, so this part of heat loss is often ignored, and heat conduction and heat convection are used as heat transfer methods.

Since the cooling process of the mold in injection molding is

influenced by various aspects such as material, process and mold, the phenomenon of mold heat transfer is intricate and complex, and it is difficult to describe it accurately through mathematical or physical models. We make the following reasonable assumptions and simplifications in our study:

1. The mold is in a steady state of production with a constant average temperature throughout the molding cycle.
2. Heat transfer within the plastic part is simplified as a one-dimensional transient process, occurring solely along the normal direction of the cavity surface.
3. The plastic part is assumed to be in perfect contact with the mold cavity surface, with zero contact thermal resistance.
4. Heat transfer inside the mold is considered to be governed by conduction and convection, disregarding external heat dissipation and heat transfer to the injection molding machine table.
5. The thermal properties of the plastic, mold, and coolant (such as specific heat capacity, thermal conductivity, density, etc.) are assumed to be constant and independent of temperature changes.

These assumptions provide a simplified framework for our analysis while maintaining a reasonable level of accuracy.

3.2 Building the mathematical model

3.2.1 Analysis of heat transfer inside the mold

When the melt fills the mold cavity, its flow behavior is a

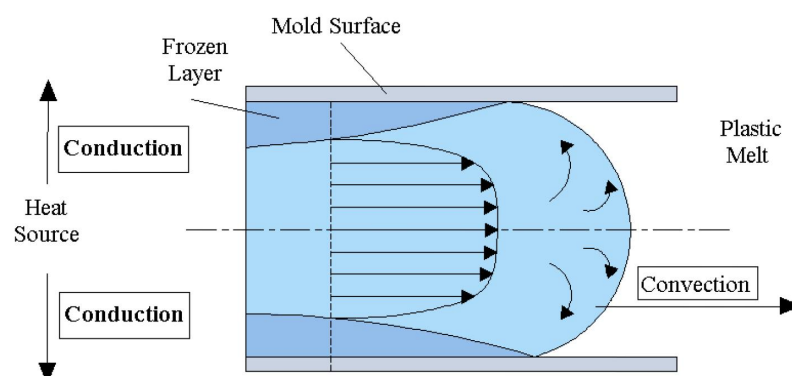


Figure 6 The heat transfer behavior of molten material during flow

three-dimensional transient heat transfer process. As shown in Fig. 6, when the mold cavity is filled, the plastic melt first advances rapidly in the form of fountain flow driven by the injection pressure, and the flow end of the high-temperature melt continuously contacts with the colder mold wall to form a solidified layer by phase change and transfer heat to the mold wall by heat convection and heat conduction; until the end of filling, the central layer of the high-temperature melt is always transferring heat to the low-temperature cavity wall. Until the end of filling, the high temperature melt center layer is always transferring heat to the low temperature cavity wall, so that the liquid melt becomes a solid plastic part.

It is a nonlinear heat conduction problem, which is much more complicated than the simple heat conduction problem, and the mathematical description of this process is more complicated to be accurate. Since the thickness direction of the plastic part is much smaller than the length and width of the plastic part, we simplify the mathematical model according to this principle by assuming that the direction of heat transfer of the plastic part is only along the normal direction of the cavity surface, which is simplified to a one-dimensional phase change heat transfer. It can be considered as a one-dimensional solidification process of the plastic, and the study is divided into two regions: the liquid phase region and the solid phase region. The phase change temperature is T_p . The phase change process starts at T and then advances to its interior until the phase change is fully completed. During the phase transition, the phase interface moves along the x-axis and its

position is a function of time $s(t)$.

Due to the short time of melt injection to fill the cavity, the convective heat conduction in the melt is negligible. Using $T_s(x, t)$ and $T_l(x, t)$ to denote the temperatures in the solid and liquid phase regions, then the differential equations for the thermal conductivity of the solid and liquid phases are

$$\frac{\partial T_s}{\partial t} = \alpha_s \frac{\partial^2 T_s}{\partial x^2}, 0 \leq x \leq s(t) \quad (3-1)$$

$$\frac{\partial T_l}{\partial t} = \alpha_l \frac{\partial^2 T_l}{\partial x^2}, s(t) < x \quad (3-2)$$

where, α is the thermal diffusion coefficient, m^2/s . $\alpha = \lambda/c\rho$, where, λ is the thermal conductivity, $kW/m \cdot ^\circ C$. c is the specific heat capacity, $kJ/(kg \cdot ^\circ C)$. ρ is the density, kg/m^3 .

At the interface of the two phases, we can obtain

$$T_s(x, t) = T_l(x, t) = T_p, x = s(t) \quad (3-3)$$

According to the law of conservation of energy, the heat released by the phase change process has

$$Q_1 = \lambda_s \frac{\partial T_s}{\partial x} - \lambda_l \frac{\partial T_l}{\partial x} = \rho_p L \frac{ds(t)}{dt} \quad (3-4)$$

where, ρ_p is the density of the plastic part; L is the latent heat of phase change per unit mass of the material; and λ is the thermal conductivity.

3.2.2 Cooling channels convective heat transfer model

When the coolant is forced to flow into the circular channel at a uniform flow rate and Re is greater than the critical value, a turbulent boundary layer will gradually develop on the boundary of the channel and finally converge in the center of the channel to reach the fully turbulent development zone.

Assume that the coolant moves in the channel of length L and the wall temperature T_W is kept constant. The temperature at the coolant inlet is

T_f , the temperature at the outlet is $T_{f'}$, and the average flow velocity is u . Fig. 7 is a schematic diagram showing the heat balance of the cooling fluid in the micro-element control volume with length dx .

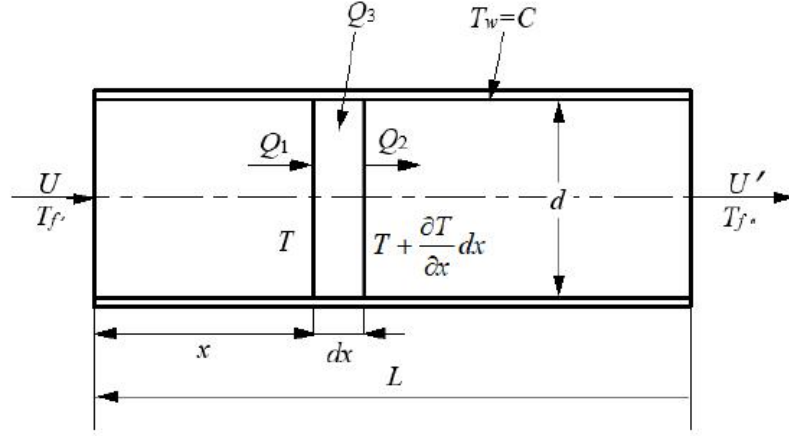


Figure 7 Schematic diagram of thermal equilibrium of a cooling channel element with length dx

The cross-sectional average temperature of the fluid at any cross-section at a distance x from the inlet is T . The heat flow into the micro-element is

$$Q_1 = \frac{\pi}{4} \rho d^2 u c T \quad (3-5)$$

where, ρ is the density of coolant and c is the specific heat capacity of coolant.

The heat flow out of the micro element is

$$Q_2 = \frac{\pi}{4} \rho d^2 u c \left(T + \frac{dT}{dx} dx \right) \quad (3-6)$$

The heat flow from the wall to the micro-element is

$$Q_3 = h(\pi d \cdot dx)(T_w - T) \quad (3-7)$$

According to the equation

$$Q_2 - Q_1 = Q_3 \quad (3-8)$$

We can obtain

$$\rho d^2 u c dT = 4hd(T_w - T)dx \quad (3-9)$$

Separating the variables yields

$$\frac{dT}{T_w - T} = \frac{4h}{\rho u c} \cdot \frac{dx}{d} \quad (3-10)$$

The boundary conditions are: When $x = 0$, $T = T_{f'}$; When $x = x$, $T = T_f$. Integrating the above equation yields the temperature variation law of the coolant along the tube axis as

$$\frac{T_w - T}{T_w - T_{f'}} = \exp\left(\frac{4h}{\rho u c} \cdot \frac{x}{d}\right) = \exp\left(-4St \frac{x}{d}\right) \quad (3-11)$$

When $x = L$, $T = T_{f''}$ and T is equal to the average temperature of the coolant outlet section, so

$$\frac{T_w - T_{f''}}{T_w - T_{f'}} = \exp\left(-4St \cdot \frac{L}{d}\right) \quad (3-12)$$

As for the convective heat transfer between the coolant and the mold, it boils down to the question of how to determine the heat transfer coefficient. When $Re > 10000$, $0.5 < Pr < 120$, $L/d > 50$, heat transfer of the turbulent flow in the tube has $Nu_{d,f} = 0.027 Re_{d,f}^{0.8} Pr_f^{1/3} \left(\frac{\mu_f}{\mu_w}\right)^{0.14}$

In the formula, μ_w is the viscosity of the cooling liquid when the wall temperature is T_w , and other physical parameters are determined by the average temperature of the cooling liquid.

Nu is the Nusselt number, which can be regarded as the ratio of the convective heat transfer heat flow on the wall of the coolant channel to the heat conduction heat flow of the fluid:

$$Nu = \frac{hl}{\lambda} = \frac{h\vartheta}{\left(\frac{\lambda}{l}\right)\vartheta} \quad (3-13)$$

In the formula, l is the length representing the heat transfer area, and $l = d$ in this model.

Re is the Reynolds number, defined as

$$Re = \rho u \frac{d}{\mu} \quad (3-14)$$

Finally, the cooling liquid convective heat transfer equation is obtained as

$$\frac{hd}{\lambda_f} = 0.027 \left(\frac{\rho u d}{\mu} \right)_f^{0.8} \left(\frac{\mu c}{\lambda} \right)_f^{\frac{1}{3}} \left(\frac{\mu_f}{\mu_w} \right)^{0.14} \quad (3-15)$$

3.2.3 Heat transfer model of the mold

According to the above assumptions and simplifications, we believe that all the heat released from the plastic melt is carried away by the coolant. Then the energy equation can be simplified as

$$Q_P = Q_M = Q_C \quad (3-16)$$

where the heat of the plastic melt transfer coolant can be calculated as

$$Q_p = 10^{-3} [(T_M - T_E) c_P] \rho_p \frac{\delta}{2} l \quad (3-17)$$

where, δ is the thickness of the plastic part, l is the center distance of the adjacent cooling channel.

The heat transferred by the heat exchange between the mold and the coolant can be calculated by

$$Q_C = 10^{-3} t_c \left(\frac{1}{10^{-3} \alpha \pi d} + \frac{1}{\lambda_m S_e} \right)^{-1} (T_W - T_C) \quad (3-18)$$

where t_c is the time to reach the ejector temperature (cooling time); α is the heat transfer coefficient of the coolant; λ_m is the thermal conductivity of the die steel; S_e is the thermal conductivity shape factor.

The heat transfer coefficient of water is

$$\alpha = \frac{31.395}{d} Re^{0.8} \quad (3-19)$$

Re is the Reynolds number, defined as

$$Re = \rho u \frac{d}{\mu} \quad (3-20)$$

where, ρ is the density of coolant, u is the average flow rate of coolant in the tube, μ is the viscosity of coolant.

S_e has a length dimension and is a purely aggregated parameter whose value depends on the change around the isothermal surface along the direction of the heat flow vector and only on the shape and size of the heat conduction system. For each cooling channel in the follower-shaped

cooling model, the shape factor is:

$$S_e = \frac{2\pi}{\ln \left[\frac{2l \sin(2\pi s/l)}{\pi d} \right]} \quad (3-21)$$

Where, d is the diameter of the cooling channel, s is the distance from the centerline of the cooling channel to the surface of the cavity.

Cooling time of flat type plastic parts

$$t_c = \frac{\delta^2}{\pi^2 a} \ln \left[\frac{4}{\pi} \left(\frac{T_M - T_W}{T_E - T_W} \right) \right] \quad (3-22)$$

In the formula, a is the thermal conductivity of the plastic melt, which is defined as

$$a = \frac{\lambda_p}{\rho_p c_p} \quad (3-23)$$

The cooling time depends on the thermal properties of the plastic, the thickness of the part and the process conditions, and it is not directly related to the design parameters of the cooling channels. However, since the design configuration of the cooling channels affects the cavity temperature, it indirectly affects the cooling time.

By iterating, we can obtain:

$$\begin{aligned} & \frac{[c_p (T_M - T_E)] \rho_s \frac{\delta}{2} l}{T_W - T_C} \cdot \left\{ \frac{1}{2\pi\lambda_m} \ln \left[\frac{2l \sin\left(2\pi \frac{s}{l}\right)}{\pi d} \right] + \frac{1}{0.031395\pi \text{Re}^{0.8}} \right\} \\ & = \frac{\rho_p c_p \delta^2}{\pi^2 \lambda_p} \ln \left[\frac{4}{\pi} \left(\frac{T_M - T_W}{T_E - T_W} \right) \right] \quad (3-24) \end{aligned}$$

Therefore, the cooling time of the plastic part is:

$$t_c = \frac{[c_p (T_M - T_E)] \rho_s \frac{\delta}{2} l}{T_W - T_C} \cdot \left\{ \frac{1}{2\pi\lambda_m} \ln \left[\frac{2l \sin\left(2\pi \frac{s}{l}\right)}{\pi d} \right] + \frac{1}{0.031395\pi \text{Re}^{0.8}} \right\} \quad (3-25)$$

Due to the three-dimensional heat transfer effect, the cooling process of curved products is different from that of flat products, so the cooling effect on the inner and outer surfaces of the product is different under the same configuration of the cooling channels, and the difference in

temperature distribution between the two sides will generate residual stresses and cause warpage and deformation. Based on the above reasons, the above formula is used to find out the mold temperature, to make the minimum temperature distribution of the cavity, we have

$$\frac{1}{N} \sum_{i=1}^N (T_i)_i - \frac{1}{M} \sum_{j=1}^M (T_o)_j = 0 \quad (3-26)$$

where N and M are the number of cooling units, T_i and T_o are the temperatures of the inner and outer surfaces of the product, respectively. T_i and T_o are the temperature of the inner and outer surfaces of the product, respectively.

In summary, the mathematical models of melt heat conduction, convection heat transfer of coolant and heat transfer inside the mold were established, and the heat transfer mechanism of the cooling process was analyzed in detail. The factors affecting the cooling time and mold temperature distribution include the product wall thickness, the diameter of the cooling channels, the distance between adjacent cooling channels and the distance from the centerline of the cooling channels to the cavity.

4 DESIGN ANALYSIS OF CONFORMAL COOLING CHANNELS

The process parameters of injection molding and the design parameters of the cooling channels are the main factors affecting the cooling of the product for the conformal cooling channels. The former can obtain the best process variables through the experimental design of simulation software or obtain the better design parameters through the experience of the injection molding technician. The latter is generally based on the designer's design experience or the design specifications of traditional cooling channels. Although the design rules for traditional cooling channels in terms of channels diameter, spacing between channels, and distance from channels to cavities can be useful for 3D printing with shaped cooling channels, it is still not possible to accurately predict whether the design will result in optimal cooling for shaped channels.

To improve production efficiency and ensure product quality, the cooling system should be designed to shorten the molding cycle and evenly cool the product, which requires analysis of important design parameters that affect the cooling effect of the cooling channels. Since the design rules of the conventional cooling channels have some reference for the design of the conformal cooling channels, we analyze the design parameters of the conformal cooling channels based on the design rules of the conventional cooling channels.

Through the previous analysis, we learned that the design variables affecting the cooling effect of the conformal cooling channels are the type of channels arrangement (such as series or parallel arrangement), the cross-sectional geometry of the channels, the diameter size of the channels, the distance between adjacent channels and the distance from

the centerline of the channels to the cavity, and other factors. Since the type of channels layout and cross-sectional geometry are qualitative factors, it is difficult to conduct quantitative research, so we first conducted a single-factor experimental analysis of these two. For factors such as the diameter of the channels, the spacing of adjacent channels and the distance from the centerline of the channels to the cavity that can be quantitatively analyzed, response surface test analysis is conducted to obtain the quantitative expression of the relationship between the factors and the cooling index, and then the multi-objective optimization of the design of the conformal cooling channels.

4.1 The general principles of cooling channels design

Based on the designer's design experience or the design principles of the traditional cooling channels, the design of the conformal cooling channels has also derived several design specifications:

(1) the diameter of the channels. The diameter of the traditional cooling channels is usually between 8 ~ 12mm, too large a diameter will lead to the channels wall close to the mold parts, affecting the strength and life of the mold. If the diameter is too small, the drill bit will be easily deflected during the channels processing, causing damage to the mold. Since the manufacturing of the channels relies on 3D printing processing means, avoiding the limitations of drilling processing, and used in the traditional channels cannot be cooled in a narrow local area, so the minimum diameter of the channels than the minimum diameter of the traditional channels is smaller, as small as 1mm, commonly used with the shape of the channel's diameter is generally between 4 ~ 10 mm.

(2) The center distance of adjacent channels. The closer the distance between adjacent channels, the faster the cooling. To uniform cooling, for the heat accumulation place, the channels arrangement should be dense,

that is, the distance between the channels should be smaller. For the conformal cooling channels, in the case that the channels arrangement is not restricted, and the mold strength is guaranteed, the distance between adjacent channels should also be as small as possible.

(3) The distance from the center line of the channels to the cavity. For the wall thickness of uniform plastic parts, the parts of the plastic with the shape of the channels and the cavity surface always need to maintain the same distance, to achieve uniform cooling effect. Wall thickness of the plastic parts, wall thickness of more heat, so the channels should be closer to the thicker parts of the product cavity, as shown in Fig. 8. These principles also apply to conformal cooling channels.

(4) The cross-section of the channels. Traditional channels due to its

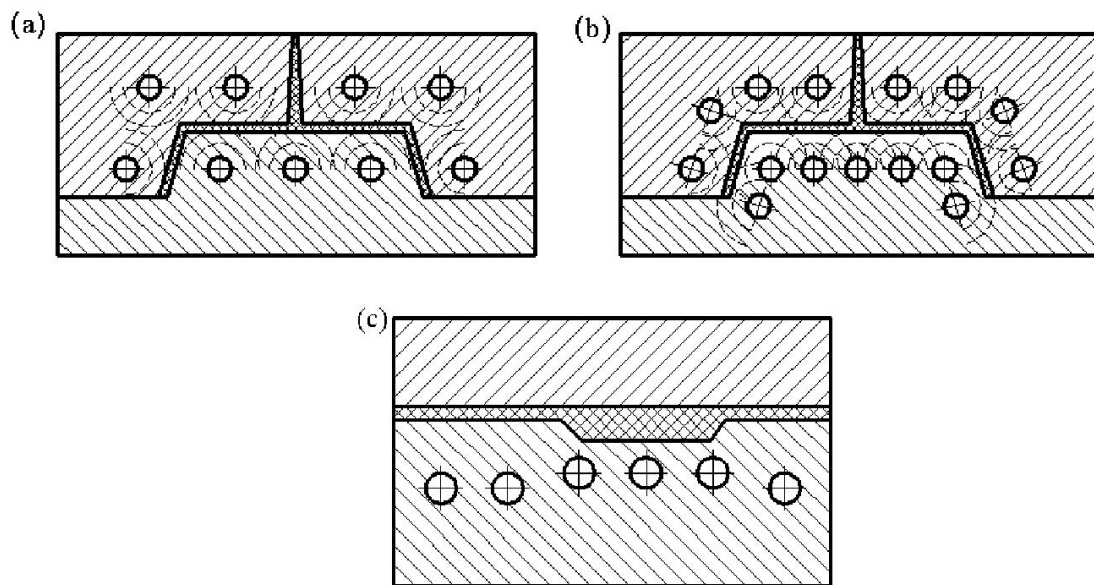


Figure 10 Schematic diagram of cooling channel layout

processing means, the channels cross-sectional size and shape almost does not change. 3D printing with the shape of the channels has flexibility, the channels cross-sectional shape can be changed according to the shape of the product, but still to maintain the same channels cross-sectional area equal to ensure a constant coolant through the channels. When the

channels is connected in parallel, that is, a channels is divided into multiple fine channels for cooling, then the sum of the cross-sectional area of the branch channels should be at least equal to the total dry channels cross-sectional area of the water inlet, to ensure the uniform flow of coolant in all parts of the channels.

(5) The length of the channels. In order to prevent the pressure drop of the channels is too large, the channels temperature is too high to produce uneven cooling, the length of the traditional cooling channels and the flow of coolant should not be too long. With the shape of the channels due to the small diameter of the channels, theoretically the length of the channels should be less than the traditional channels, so that the coolant quickly through the heat zone in time to take away the heat.

4.2 Simulation analysis of cooling channels with different configurations

To study the cooling effect of cooling channels with different cross-sectional shapes and different layout types, and to know which cross-sectional shape and layout type of the channels have a significant impact on the cooling of the product, the above problems can be effectively solved by using one-way analysis of variance (ANOVA).

4.2.1 Introduction to one-way analysis of variance

ANOVA is one of the common data processing methods in mathematical statistics. It is a data analysis and processing method used to analyze experimental data to test whether the means of multiple normal totals with equal variances are equal, and thus determine whether the effect of the factor or level on the test index is significant. In an ANOVA test, if the level of only one factor is changing, while the levels of other factors are fixed, and the purpose of the test is to compare the differences between the values of the indicators at each level of the factors, it is

called a one-way test. If the levels of two or more factors are changing, it is called a multi-factor test. In this section, a one-way ANOVA is conducted to examine the effect of cross-section geometry and type of arrangement on the cooling effect, respectively. The steps of ANOVA for one-way tests are as follows:

(1) Formulation of hypothesis

In a one-way test, there are r levels of factor A affecting the index, and each level is repeated n_i times, and the obtained test result y_{ij} represents the response value of the i -th level A_i of factor A in the j -th repeated test.

Assuming $y_{ij} \sim N(\mu_i, \sigma^2)$, there is

$$\mu_i = \mu + \alpha_i \quad (4-1)$$

Then we can obtain

$$\begin{cases} y_{ij} = \mu + \alpha_i + \varepsilon_{ij} \\ \varepsilon_{ij} \sim N(0, \sigma^2) \end{cases}, i = 1, 2, \dots, r, j = 1, 2, \dots, n_i \quad (4-2)$$

where, α_i denotes the main effect of the i -th level of factor A and μ_i denotes the total mean of the response. Then inferring whether a change in the level of factor A is significant to the response y is equivalent to testing whether the hypothesis holds. $H_0: \alpha_1 = \alpha_2 = \dots = \alpha_r = 0$, at least one of them is not zero. If the assumption holds, factor A has no significant effect on the indicator. Otherwise, factor A is considered to have a significant impact on the index.

(2) Construct the test statistic

First, defining

$$SST = \sum_{i=1}^r \sum_{j=1}^{n_i} (y_{ij} - \bar{y})^2 \quad (4-3)$$

SST indicates the total fluctuation of the corresponding value and is called the sum of squared deviations.

$$SSA = \sum_{i=1}^r n_i (\bar{y}_i - \bar{y})^2 \quad (4-4)$$

$$SSE = \sum_{i=1}^r \sum_{j=1}^{n_i} (y_{ij} - \bar{y}_i)^2 \quad (4-5)$$

SSE , SSA are called the sum of squares of errors (within-group sum of squares) and the sum of squares of deviations (between-group sum of squares) of factor A . SSE reflects the fluctuation of response values caused by the test error, while SSA reflects the fluctuation of response values caused by the change of factor A level. Then we have the formula for the decomposition of the sum of squared deviations

$$SST = SSA + SSE \quad (4-6)$$

Denoting MS as the mean sum of squares of deviations, we have:

$$MS = \frac{SS}{df} \quad (4-7)$$

where df is the sample degree of freedom, and $df_A = r - 1$, $df_E = n - r$.

The statistics F_A is:

$$F_A = \frac{MSA}{MSE} = \frac{\frac{SSA}{df_A}}{\frac{SSE}{df_E}} = \frac{\frac{SSA}{r-1}}{\frac{SSE}{n-r}} \quad (4-8)$$

The statistic is used as the statistic to test whether the hypothesis H_0 is established. It can be proved that under the condition that H_0 is established, $F_A \sim F(r - 1, n - r)$. Therefore, for a given significant test level α , the value of $F_A \sim F(r - 1, n - r)$ can be found out from the F distribution critical table, so that

$$P\{F_A \geq F_\alpha(r - 1, n - r)\} = \alpha \quad (4-9)$$

If $F_A \geq F_\alpha(r - 1, n - r)$, then H_0 is rejected, the hypothesis that different levels of factor A have a significant effect on the test results at the significant level; if $F_A < F_\alpha(r - 1, n - r)$, then H_0 is accepted, the hypothesis that different levels of factor A have no significant effect on the test results.

(3) Multiple comparisons (S-test)

If the F-test is significant, it only indicates that there is a significant difference between the levels of the factors but does not indicate which levels are significantly different from each other, so further comparisons of the levels, i.e., multiple comparisons are required.

For a given test level, we can calculate

$$D_{ij}(\alpha) = \sqrt{\left(\frac{1}{n_i} + \frac{1}{n_j}\right) \frac{S_e^2}{n-r} (r-1) F_{\alpha}(r-1, n-r)} \quad (4-10)$$

After calculating the value of $D_{ij}(\alpha)$, when $|\bar{y}(i) - \bar{y}(j)| \leq D_{ij}(\alpha)$, it is considered that the difference between A_i and A_j is not significant at level α . Otherwise, the difference is considered significant. Among them, $\bar{y}(i)$ represents the i -th arrangement of the average value of indicators at each level from large to small, and $\bar{y}(j)$ represents the j -th arrangement of the average value of indicators at each level from small to large. A_i and A_j represent the levels corresponding to $\bar{y}(i)$ and $\bar{y}(j)$ respectively.

4.2.2 The influence of the cross-sectional shape of cooling channels on cooling effectiveness

It is known from the geometric principle that when the cross-sectional area of the cooling channel is certain, the perimeter of the cooling channel with different cross-sectional shapes is the smallest in the circular section. Therefore, theoretically, in the mold heat transfer process, when the cross-sectional area of the cooling channel is certain, the cooling channel length is equal, compared to other cross-sectional shape of the cooling channel, the cooling channel with a circular cross-section has a smaller heat transfer area. Previous studies in the literature have studied semi-circular, circular, U-shaped, and rectangular cross-sectional cooling channels, but the cross-sectional objects studied are too theoretical and not common in production practice, so the guidance for engineering

applications is small.

To examine the cooling effect of different cross-sectional shapes of cooling channels commonly used in engineering applications, this section analyzes and compares the results of simulation of cooling channels with round and elliptical cross-sections commonly used in daily production.

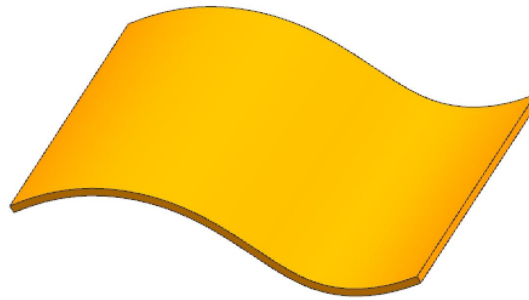


Figure 9 Plastic part structure

To avoid the design and modeling errors of the water channel and make the test results accurate and reliable, this section selects a more idealized curved thin surface product for the study of the cross-sectional shape of the conformal cooling channel, as shown in Fig. 9. The wall thickness of the product is 1.5 mm, and the size is 80×80 mm. Moldflow transient heat transfer is used to simulate the cooling results, and the injection molding process parameters are shown in Table 1.

Table 1 Injection molding process parameters

| Process Item | Parameter |
|----------------------|-----------|
| Injection Time | 0.3s |
| Melt Temperature | 210°C |
| Mold Temperature | 60°C |
| Holding Time | 3s |
| Cooling Time | 5s |
| Ejection Temperature | 80°C |

(1) Modeling cooling channels

The model established for the test is shown in Fig. 10, there are two models of cooling channel arrangement are parallel cooling channel type, cooling channel spacing l for 18mm, cooling channel centerline to the distance of the cavity s for 12mm. cross-sectional circle diameter d for 6mm, the ellipse long semi-axis a for 5mm, short semi-axis b for 1.8mm, both of which have an area of $9\pi \text{ mm}^2$, ensuring equal flow rate of coolant per unit time at the same flow rate.

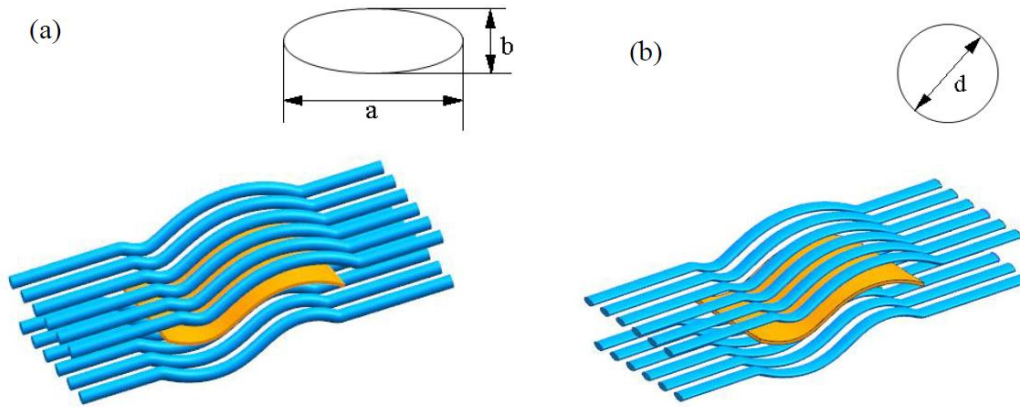


Figure 10 The model of cooling channels with different cross-section shapes

(2) Single-factor test design

In this single-factor test, we took cooling time and product cooling uniformity as the test indexes, and only took two levels of circular and elliptical sections of the conformal cooling channel for comparison. The effect of different cross-sectional shapes on the cooling effect was investigated. We note the cross-sectional geometry of the cooling channel as factor A , the number of level of factor A is $r = 2$, circular and elliptical cross-section as level A_1 , A_2 , respectively, the number of repetitions under each level is $n_i = 3$.

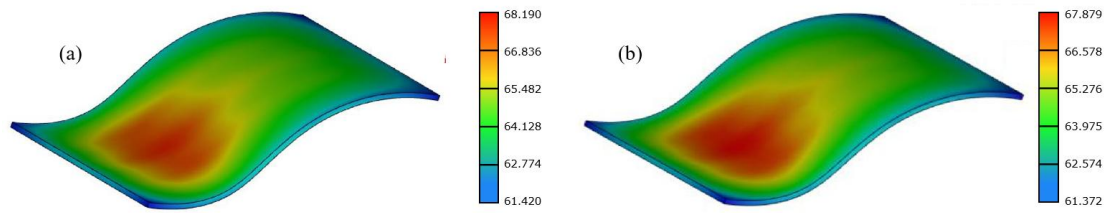


Figure 11 Temperature distribution of products at the end of cooling

The cooling time is defined as the time from the start of product injection to the time when the product reaches the ejection temperature, and the product cooling uniformity is defined by the extreme difference of the product surface temperature at the time when the ejection temperature is reached.

Table 2 Simulation Results of different cross-sectional shape

| Cross-sectional Shape | Cooling Time/s | | | Cooling Uniformity/°C | | |
|-----------------------|----------------|-------|-------|-----------------------|-------|-------|
| | 1 | 2 | 3 | 1 | 2 | 3 |
| Circular | 6.088 | 6.090 | 6.114 | 6.705 | 6.686 | 6.770 |
| Elliptical | 6.012 | 6.034 | 6.098 | 6.361 | 6.403 | 6.507 |

(3) Analysis of test results

Conduct statistical analysis on the test data, and get the test data calculation table as shown in Table 3 and Table 4. The analysis of variance table for the significance test after calculating the statistics is shown in Table 5 and Table 6.

Table 3 Data analysis (cooling time)

| Cross-section | 1 | 2 | 3 | Σ | $\frac{1}{m_i}\Sigma^2$ | Σ^2 | \bar{y}_i |
|---------------|-------|-------|-------|----------|-------------------------|------------|-------------|
| Circular | 6.088 | 6.090 | 6.114 | 18.292 | 111.532 | 111.532 | 6.097 |
| Elliptical | 6.012 | 6.034 | 6.098 | 18.144 | 109.735 | 109.739 | 6.048 |
| Σ | | | | 36.436 | 221.267 | 221.271 | 12.145 |

Table 4 Data analysis (uniformity of mold temperature distribution)

| Cross-section | 1 | 2 | 3 | Σ | $\frac{1}{m_i}\Sigma^2$ | Σ^2 | \bar{y}_i |
|---------------|-------|-------|-------|----------|-------------------------|------------|-------------|
| Circular | 6.705 | 6.686 | 6.770 | 20.161 | 45.164 | 135.492 | 6.720 |
| Elliptical | 6.361 | 6.403 | 6.507 | 19.271 | 41.267 | 123.801 | 6.424 |
| Σ | | | | 39.432 | 259.294 | 259.294 | 13.144 |

Table 5 Variance analysis table (cooling time)

| Source of variation | SS | df | MS | F | P-value | Significance |
|---------------------|---------|----|---------|-------|---------|--------------|
| Treatment | 0.00365 | 1 | 0.00365 | 3.311 | 0.143 | |
| error | 0.00441 | 4 | 0.00110 | | | |
| total | 0.00806 | 5 | | | | |

Table 6 Variance analysis table (mold temperature distribution uniformity)

| Source of variation | SS | df | MS | F | P-value | Significance |
|---------------------|--------|----|-------|--------|---------|--------------|
| Treatment | 0.132 | 1 | 0.132 | 34.789 | 0.004 | ** |
| error | 0.0152 | 4 | 0.004 | | | |
| total | 0.147 | 5 | | | | |

Note: In the column of significance, if $\alpha = 0.05$, the test result is significant, then mark *. For $\alpha = 0.01$, if the test result is significant, mark **.

In summary, the change of the cross-sectional shape of the cooling channel has basically no effect on the cooling time of the product and has a certain effect on the cooling uniformity of the product, but the effect is small. In actual production, although 3D printing can produce any cross-sectional cooling channel of any shape, but compared with other cross-sectional cooling channels, the circular cooling channel is easy to control the flow state, the channel pressure loss is minimal, and the strength of the circular side of the cooling channel cross-section is greater

than the strength of the flat side, the circular cooling channel can ensure better mold strength. Therefore, in the case that there is no restriction on the design of the cooling channel cross-section, circular is preferred in the design of the conformal cooling channel.

4.2.3 The effect of the type of cooling channel arrangement on the cooling effect

The conventional cooling channels is divided into two types: series and parallel, where the series cooling channels usually shows a Z-shaped arrangement and spiral arrangement, parallel cooling channels shows a parallel arrangement is shown in Fig. 12. In these two types of circuits, the amount of heat removed by the coolant is determined by the heat input from the plastic melt, the heat transfer efficiency of the mold and the flow state of the coolant.

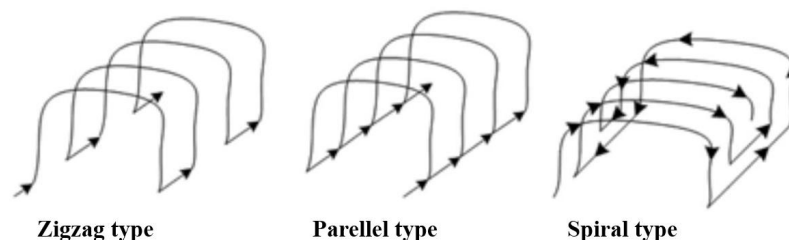


Figure 12 Layout type of cooling channels

When the cooling channels is connected in series, the cooling channels should not be too long, and the temperature difference between the inlet and outlet should not exceed 3°C. This is because when the water flow is too long, it will lead to a gradual increase in the temperature of the coolant along the direction of flow, resulting in excessive differences in temperature in the same cooling channel, which is not conducive to uniform cooling of the product. Too long water flow will also lead to higher resistance to flow, while easy to accumulate scale caused by water blockage. When the cooling channels in parallel, can solve the cooling

channels too large process problems, but because the parallel cooling channels usually from a main road branch into multiple branches, and

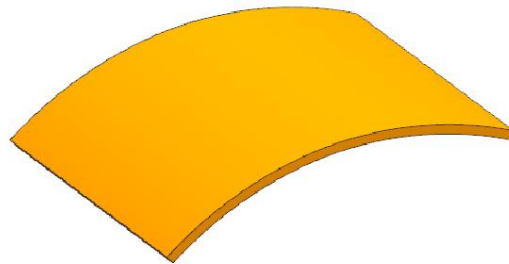


Figure 13 Plastic part B structure

then converge into cooling channels, so the cooling channels requires a larger flow of coolant, but also difficult to ensure that each branch fluid flow, flow rate and flow state consistent, which may cause uneven cooling of the product.

To examine the cooling effect of different types of arrangement with the shape of the cooling channel, this section analyzes and compares the simulation results of the Z-shaped, parallel, mesh, and spiral cooling channel layouts that are commonly used in daily production or scientific research.

To reduce the modeling error, this section still uses the idealized curved sheet plastic parts for the study. Fig. 13 shows the plastic part selected for the study of the cooling channel layout type, with a wall thickness of 2

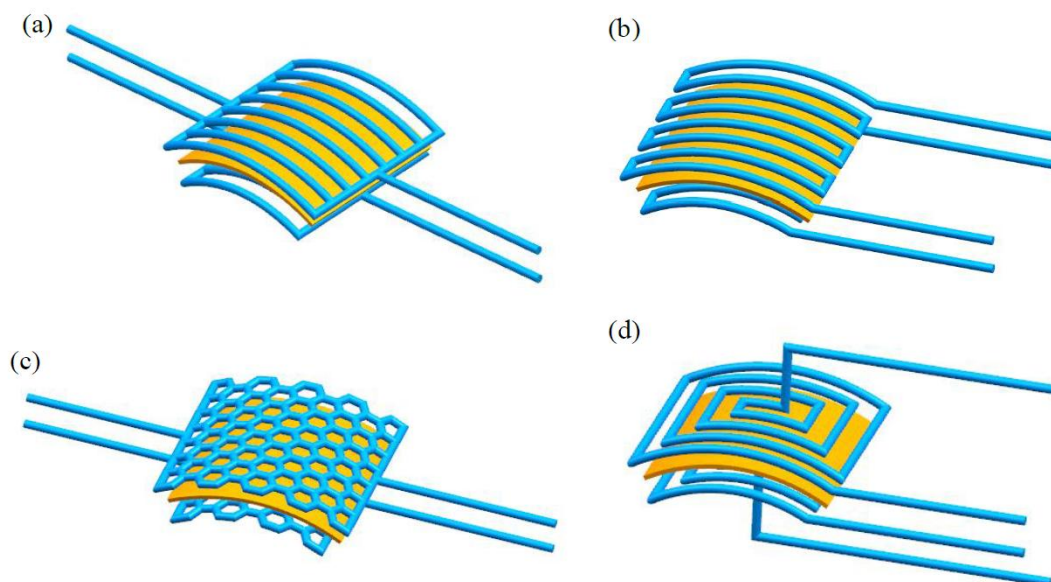


Figure 14 Cooling channel models with different layout

mm and dimensions of 80×80 mm.

(1) Cooling channels model

Fig. 14 is the cooling channel model established by the test, and a-d are the Z-shaped, parallel, mesh-shaped, and spiral-shaped cooling channel layouts in turn. Each cooling channel has only one water inlet and one water outlet, the diameter d is 4mm, the equivalent distance l between the cooling channels is 10mm, and the distance s from the centerline of the cooling channel to the cavity is 8mm.

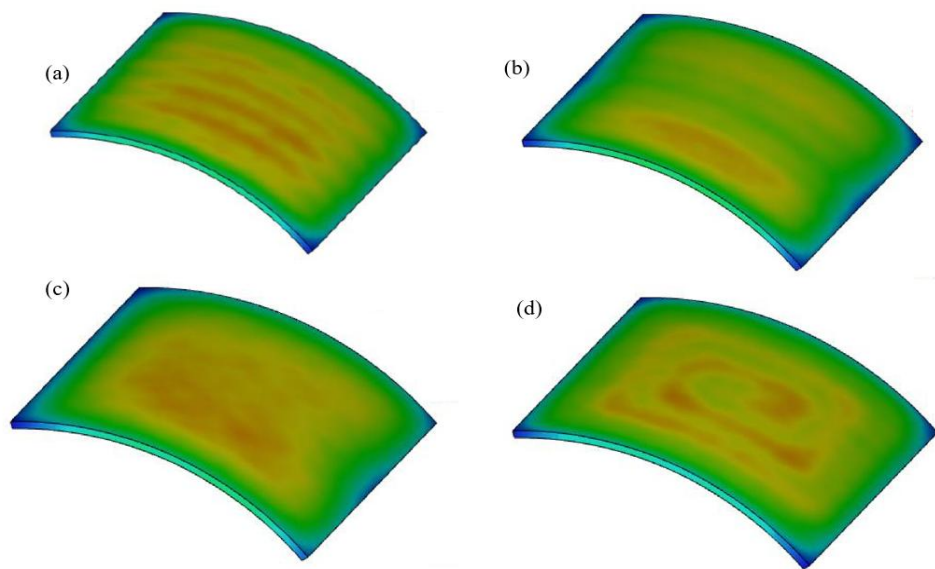


Figure 15 Temperature distribution of products at the end of cooling

(2) Single-factor test design

Since the cooling effect of the cooling water channels arranged in series is better than that of the parallel arrangement, for general curved surface products, the cooling water channels arranged in series are preferred, that is, the spiral or Z-shaped arrangement. Among them, products with curvature and spherical surface are suitable for spiral arrangement, and products with smaller sizes are suitable for Z-shaped arrangement. When the shape of the product is special and the above two arrangements of cooling channels cannot be used, a parallel arrangement can be considered, that is, a parallel arrangement of conformal cooling

channels or a mesh arrangement.

Table 7 Simulation results

| Cross-section | Cooling Time/s | | | Cooling Uniformity/°C | | |
|---------------|----------------|-------|-------|-----------------------|-------|-------|
| | 1 | 2 | 3 | 1 | 2 | 3 |
| Z-shaped | 7.896 | 7.888 | 8.111 | 4.483 | 4.590 | 4.641 |
| Parallel | 8.472 | 8.375 | 8.455 | 6.563 | 6.686 | 6.585 |
| Mesh type | 8.292 | 8.281 | 8.282 | 6.698 | 6.613 | 6.457 |
| Spiral | 7.989 | 8.013 | 8.026 | 4.791 | 4.693 | 4.611 |

(3) Analysis of test results

Statistical analysis was carried out on the test data, and the calculation of the test data was obtained as shown in Table 8 and Table 9. After statistical calculation, the significance test is shown in Table 10 and Table 11.

Table 8 Data analysis (cooling time)

| Level | 1 | 2 | 3 | Σ | $\frac{1}{m_i}\Sigma^2$ | Σ^2 | \bar{y}_i |
|-----------|-------|-------|-------|----------|-------------------------|------------|-------------|
| Z-shaped | 7.896 | 7.888 | 8.111 | 23.895 | 190.324 | 190.356 | 7.965 |
| Parallel | 8.472 | 8.375 | 8.455 | 25.302 | 213.397 | 213.402 | 8.434 |
| Mesh type | 8.292 | 8.281 | 8.282 | 24.855 | 205.924 | 205.924 | 8.285 |
| Spiral | 7.989 | 8.013 | 8.026 | 24.028 | 192.448 | 192.449 | 8.009 |
| Σ | | | | 98.080 | 802.092 | 802.131 | 32.693 |

Table 9 Data analysis (cooling uniformity)

| Level | 1 | 2 | 3 | Σ | $\frac{1}{m_i}\Sigma^2$ | Σ^2 | \bar{y}_i |
|-----------|-------|-------|-------|----------|-------------------------|------------|-------------|
| Z-shaped | 4.483 | 4.590 | 4.641 | 13.714 | 62.691 | 62.704 | 4.571 |
| Parallel | 6.563 | 6.686 | 6.585 | 19.834 | 131.129 | 131.138 | 6.611 |
| Mesh type | 6.698 | 6.613 | 6.457 | 19.768 | 130.258 | 130.288 | 6.589 |
| Spiral | 4.791 | 4.693 | 4.611 | 14.095 | 66.223 | 66.239 | 4.698 |
| Σ | | | | 67.411 | 390.301 | 390.369 | 22.470 |

Table 10 Variance analysis table (cooling time)

| Sources of variation | SS | df | MS | F | P | Significance |
|----------------------|----------|----|----------|----------|----------|--------------|
| Treatment | 0.452146 | 3 | 0.150715 | 31.60424 | 8.74E-05 | ** |
| Error | 0.038151 | 8 | 0.004769 | | | |
| Total | 0.490297 | 11 | | | | |

Table 11 Variance analysis table (uniformity of mold temperature distribution)

| Sources of variation | SS | df | MS | F | P | Significance |
|----------------------|----------|----|----------|----------|----------|--------------|
| Treatment | 11.61449 | 3 | 3.871497 | 457.2679 | 2.77E-09 | ** |
| Error | 0.067733 | 8 | 0.004 | | | |
| Total | 11.68222 | 11 | | | | |

According to Table 8 and Table 9, the critical value $F_{0.05}(3,8) = 4.066$, the statistic $F = 31.406 > F_{0.05}(2,4)$, and with $P = 8.74 \times 10^{-5} < 0.05$ in the F-test, so the hypothesis H_0 is rejected. Therefore, we can conclude that at a significance level of $\alpha = 0.05$, different levels of factor B have a significant impact on the experimental results. In other words, different layouts of the conformal cooling channels have a significant effect on both the cooling time and the uniformity of product cooling. The experimental results reveal that the response values for levels B_1 and B_4 are significantly better than those for levels B_2 and B_3 . This indicates that compared to the mesh type and parallel layouts of cooling channels, the Z-shaped and spiral layouts exhibit superior performance in terms of cooling time and temperature uniformity.

Table 12 Significant differences among different levels

| Cooling Channels Layout Type | Mean Difference | Standard Error | Significance | 95% Confidence Interval | | |
|------------------------------|-----------------|----------------|--------------|-------------------------|-------------|---------|
| | | | | Upper Limit | Lower Limit | |
| B1 | B2 | -2.04000* | 0.07513 | 0.000 | -2.2132 | -1.8668 |
| | B3 | -2.01800* | 0.07513 | 0.000 | -2.1912 | -1.8448 |
| | B4 | -0.12700 | 0.07513 | 0.129 | -0.3002 | 0.0462 |
| B2 | B1 | 2.04000* | 0.07513 | 0.000 | 1.8668 | 2.2132 |
| | B3 | .02200 | 0.07513 | 0.777 | -0.1512 | 0.1952 |
| | B4 | 1.91300* | 0.07513 | 0.000 | 1.7398 | 2.0862 |
| B3 | B1 | 2.01800* | 0.07513 | 0.000 | 1.8448 | 2.1912 |
| | B2 | -0.02200 | 0.07513 | 0.777 | -0.1952 | 0.1512 |
| | B4 | 1.89100* | 0.07513 | 0.000 | 1.7178 | 2.0642 |
| B4 | B1 | 0.12700 | 0.07513 | 0.129 | -0.0462 | 0.3002 |
| | B2 | -1.91300* | 0.07513 | 0.000 | -2.0862 | -1.7398 |

| | | | | | |
|----|-----------|---------|-------|---------|---------|
| B3 | -1.89100* | 0.07513 | 0.000 | -2.0642 | -1.7178 |
|----|-----------|---------|-------|---------|---------|

Through multiple comparisons conducted using SPSS, Table 12 displays the results of significant differences between levels. It can be observed that there are significant differences between B_1 and B_4 , as well as between B_2 and B_3 . However, the differences between B_1 and B_4 , and between B_2 and B_3 are not substantial. This indicates that the Z-shaped and spiral layouts of the cooling channels yield similar cooling effects for the product.

In conclusion, the serial layout of cooling water paths outperforms the parallel layout. Therefore, for general curved products, we recommend prioritizing the serial layout, specifically the spiral or Z-shaped arrangement. The spiral layout is suitable for products with curvature and spherical surfaces, while the Z-shaped layout is more appropriate for smaller-sized products. If the product has a unique shape that cannot accommodate either of these two layouts, the parallel layout can be considered, either by arranging conformal cooling water paths in parallel or using a grid layout based on the shape.

5 MULTI-OBJECTIVE OPTIMIZATION FOR THE DESIGN OF CONFORMAL COOLING CHANNELS

Conformal cooling channels are generally used in commonly used curved surface products or local areas where conventional channels are not easy to cool. Therefore, for the investigation of cooling effects, in addition to the cross-sectional geometry of the channels and the layout of the channels, the cross-section of the channels must also be considered. There are several factors such as size, spacing between channels, distance from channels to cavity, etc.

Improving the average temperature of the cavity surface can significantly reduce the cooling time. The surface temperature of the mold cavity is influenced by various design parameters of the cooling water system, including the waterway diameter d , distance l between adjacent channels, distance s from the channel centerline to the cavity, and wall thickness δ . Therefore, in order to achieve a uniform temperature distribution in the product and minimize the cooling time, the fundamental issue lies in studying the design configuration of conformal cooling water systems. Different configurations of the conformal cooling water system will result in different surface temperatures of the cavity. An optimal combination of d , l and s will lead to the shortest cooling time and the lowest product cooling non-uniformity.

In this chapter, aiming at the above optimization purposes, the multi-objective optimization of the conformal cooling water channel is carried out, and the optimization results can be used as a reference for the mold designer to design the conformal cooling channels.

5.1 Introduction to experimental optimization

Experimental optimization is an optimization method of optimal design under the guidance of optimization thought. It starts from different advantages, rationally designs the test plan, effectively controls the test interference, and scientifically processes the test data, so as to conduct a comprehensive optimization analysis and achieve the optimization goal. Experimental optimization design has become an important aspect of modern technology. Factorial design, orthogonal design, uniform design and response surface design are the most commonly used methods in experimental optimal design.

In this study, we need to consider the influence of various design parameters (such as channel layout, channel diameter, etc.) on the cooling effect (cooling time, mold temperature distribution) of the product, and we want to know which factors have significant influence and get the quantitative relationship between the design variables and the cooling effect to optimize the cooling effect. In this paper, an approach is presented to optimize the design of CCC. The research involves an initial screening of influential factors through orthogonal experiments, followed by response surface experiments to establish a mathematical model relating design variables to cooling effects. Multi-objective optimization using genetic algorithms is then employed to achieve the optimal design of the cooling channels. The experiments are conducted through simulation, and statistical analysis software such as SPSS and MATLAB are utilized for data analysis.

5.1.1 Orthogonal experiments

The orthogonal experiment is a test method created for studying multi-factor and multi-level combinations. It uses a standardized table, the orthogonal table, to design the test and select some representative

points (test conditions) from a full-scale test in order to find the better production conditions, i.e., the optimal or better test solution. Due to the orthogonality of the orthogonal table, the points selected for the test are evenly dispersed and neatly comparable. Orthogonal experiments are a statistical design technique used to efficiently explore and analyze multiple factors simultaneously with a minimal number of experiments. By systematically varying the levels of each factor according to a predetermined orthogonal array, this technique ensures that the effects of each factor can be separately evaluated without confounding interactions. Orthogonal experiments offer the following advantages:

1. Reduction in the number of experiments, resulting in time, resource, and cost savings.
2. Elimination of interaction effects, enabling the accurate identification of the individual effects of each factor on the results.
3. Comprehensive consideration of multiple factors, providing a holistic understanding of the interrelationships among the factors.
4. High reliability of results, allowing for precise measurement and quantification of the impact of each factor on the outcomes.

Orthogonal experimental design allows for the analysis of experimental results using two methods: range analysis and variance analysis. Range analysis, also known as intuitive analysis, involves calculating the range (R) of each factor to determine their relative importance. Since the range reflects the magnitude of the factor's effect, factors with a large range indicate a significant difference in the response variable among their different levels, typically indicating their primary importance. On the other hand, factors with a small range suggest a lesser difference in the response variable among their levels, typically indicating their secondary importance. Therefore, the larger the range, the more important the factor.

Range analysis provides a simple and intuitive way to determine the

relative importance of factors through a few calculations and comprehensive analysis, enabling the identification of optimal experimental conditions. However, its limitation lies in the inability to estimate the magnitude of experimental errors and assess the analysis precision. It cannot distinguish whether the observed differences among the experimental results at different levels of a factor are truly caused by the variations in the factor levels.

To overcome these limitations, variance analysis can be used. The basic principles and methods of variance analysis for multi-factor orthogonal experimental design are similar to those used in single-factor variance analysis. However, additional calculations of sum of squares and degrees of freedom for multiple factors are required, and separate analyses, tests, and inferences need to be conducted for each factor. To compensate for these shortcomings of the visual analysis method, ANOVA can be used. The basic idea and method of ANOVA for multi-factor orthogonal tests are basically the same as that of one-way ANOVA, except that the squared deviations and degrees of freedom of several more factors need to be calculated, and each factor needs to be analyzed, tested and inferred separately.

5.1.2 Response surface methodology

Response Surface Methodology (RSM) is an experimental statistical method to obtain certain data through a reasonable experimental design method, and to fit the function relationship between factors and response values by using a quadratic polynomial regression equation. It is also called regression design because it is an experimental statistical method to find the optimal parameter variables by analyzing the regression equation. It can study the interaction between response and multiple factors and nonlinear relationship, and compared with orthogonal

experiments, RSM has fewer tests and more accurate results.

The common RSM includes two types of experimental designs, the Central Composite Design (CCD) and the Box-Behnken Design (BBD). Among them, CCD design is sequential and has higher prediction efficiency, but it also requires higher test conditions, it needs to be composed of factorial test points, central test points and axial test points, and the tests include combinations of vertex levels or combinations above vertex levels. The BBD test is a good choice when the cost of the test is too expensive or practical constraints make it impossible to test the combination of factor levels represented by the vertices.

5.1.3 Genetic algorithm for multi-objective optimization

In the field of practical engineering and scientific research, it is often necessary to face the problem of optimizing multiple objectives under certain constraints in the same system at the same time, and this kind of optimization problem containing multiple objectives and multiple constraints is called multi-objective optimization problem. According to the pairwise theory, it is known that maximization and minimization optimization problems can be transformed into each other, so the multi-objective optimization problem is equivalent to the multi-objective minimization problem. The optimal solution of a multi-objective optimization problem is often not unique, and there are generally conflicting relationships between multiple optimization objectives. A solution may be the best for a certain objective function, but not the best for other objective functions, and may even make other objectives deteriorate while optimizing a certain objective. Therefore, it is difficult to find a solution that makes all the objective functions optimal at the same time. The solution of this type of problem is to come up with a set of solutions that optimize the performance balance among multiple

objectives. These solutions are not comparable with each other in terms of the overall objective function, and their solution sets are called Pareto optimal Solutions.

Genetic Algorithms (GA) is a search algorithm based on the principle of natural selection and natural genetic mechanism. It is an optimization algorithm that simulates the natural selection, crossover and variation processes in biological genetics and evolution, and obtains an optimal or quasi-optimal solution through adaptive population search techniques. Genetic algorithm is an optimization algorithm inspired by natural selection and evolutionary processes, aiming to find optimal or near-optimal solutions through adaptive population search techniques. Among them, the Non-dominated Sorting Genetic Algorithm II (NSGA-II)

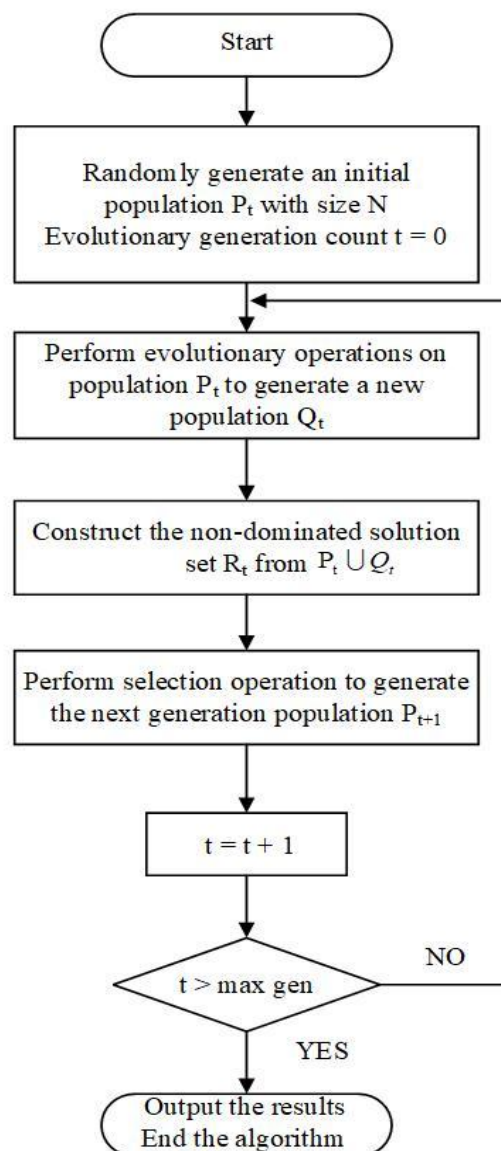


Figure 16 NSGA-II procedure flowchart

with elitist strategy is one of the most popular multi-objective optimization algorithms based on Pareto optimal front. It has high solving efficiency and can produce multiple high-quality solutions in a single run, serving as a benchmark algorithm for performance comparison with other multi-objective optimization algorithms.

This algorithm employs fast non-dominated sorting and crowding distance operator to select individuals. It uses genetic algorithm's selection, crossover, and mutation operators to generate new offspring populations. The parent and offspring populations are then combined to form a new population, and this process is repeated iteratively to generate the Pareto optimal solution set.

The basic flowchart of NSGA-II is shown in Fig. 16, and its specific steps are as follows:

Step 1: Determine the evolutionary parameters: population size M , crossover probability P_c , mutation probability P_m , and the maximum number of evolutionary iterations gen . Randomly create an initial population $P_t(t = 0)$ of N individuals, which serves as the parent population.

Step 2: Perform binary tournament selection, crossover, and mutation operations on the parent population P_t to generate a child population Q_t of size N .

Step 3: Generate a merged population $R_t = Q_t \cup P_t$ of size $2N$. Perform fast non-dominated sorting and crowding distance calculation on the merged population R_t . Based on the non-dominated ranks and crowding distances of individuals, select the best individuals to form a population P_t of size N , which will be used as the parent population for the next generation evolution.

Step 4: Check if the iteration count t has reached the maximum predefined value. If it has reached, terminate the algorithm and output the

final result. Otherwise, go back to step 2 and continue the execution.

The NSGA-II algorithm utilizes non-dominated sorting and crowding distance to maintain diversity and balance in the solution set for multi-objective optimization problems. It is capable of generating multiple high-quality non-dominated solutions.

5.2 Screening of optimization variables

When there are many factors in the test, how to filter out a few important factors from the many factors as the object of study, it is necessary to conduct screening tests, which can usually be carried out using orthogonal tests or uniform designs, etc. In the previous section, we analyzed the effect of the type of arrangement and cross-sectional geometry of the cooling channel on the cooling effect. For factors that can be quantified, such as the diameter of the cooling channel, the spacing between adjacent cooling channels and the distance from the centerline of the cooling channel to the cavity, the next orthogonal test is used to examine whether their influence on the index is significant and the respective degree of influence, to determine the test factors for the response surface test.

We use the mold cavity temperature y as the test index, and take the cooling channel diameter d , the center distance l between adjacent cooling channels, and the distance s from the center line of the cooling channel to the cavity as factors, and take three levels for each factor. The range of factor values is taken from the design guidelines proposed by Mayer in the EOS white paper as a reference, as shown in Table 13.

Table 13 The range of design variables for different wall thicknesses of channels

| Part Thickness (mm) | d (mm) | l (mm) | s (mm) |
|------------------------|----------|-----------|-------------|
| 0-2 | 4-8 | $(2-3) d$ | $(1.5-2) d$ |
| 2-4 | 8-12 | $(2-3) d$ | $(1.5-2) d$ |

| | | | |
|-----|-------|-----------|-------------|
| 4-6 | 12-14 | (2-3) d | (1.5-2) d |
|-----|-------|-----------|-------------|

The orthogonal test scheme and test results are shown in Table 14, and the variance analysis of the test results is shown in Table 15.

Table 14 Orthogonal test plan and results

| Test No. | d | l | $the s$ | yT |
|----------|-----|-----|---------|-------|
| 1 | 4 | 12 | 8 | 63.14 |
| 2 | 4 | 18 | 12 | 68.04 |
| 3 | 4 | 24 | 16 | 72.79 |
| 4 | 6 | 12 | 12 | 66.60 |
| 5 | 6 | 18 | 16 | 71.34 |
| 6 | 6 | 24 | 8 | 64.80 |
| 7 | 8 | 12 | 16 | 70.30 |
| 8 | 8 | 18 | 8 | 63.65 |
| 9 | 8 | 24 | 12 | 68.17 |

Table 15 Analysis of variance table

| Source of variance | Sum of square | Degrees of freedom | Mean square | F | Critical value | Significance |
|--------------------|---------------|--------------------|-------------|----------|----------------|--------------|
| d | 0.591 | 2 | 0.296 | 13.227 | 19.0 | |
| l | 5.457 | 2 | 2.728 | 122.107 | 19.0 | * |
| s | 86.953 | 2 | 43.477 | 1945.744 | 19.0 | * |
| Error | 0.045 | 2 | 0.022 | | | |
| Total | 41279.042 | 9 | | | | |

Note: $R_2 = 1.000$ (After adjusted, $R_2 = 0.998$)

It can be seen from Table 15 that within the existing factor level range, both factors l and s have $F > F_{\alpha}(2,2) = 19.0$, it can be seen that the distance between the center of the adjacent cooling channel and the distance from the centerline of the cooling channel to the cavity has a significant impact on the mold cavity temperature. and for factor d , we have $F > F_{0.1}(2,2) = 9.00$, obviously d passed the significance test of

$a = 0.1$, so it can be considered that the diameter of the water channel has a certain effect on the mold cavity temperature impact. The significance of an orthogonal test factor is related to its corresponding level value range. For a factor, the greater the level value range of the factor, the significance of the factor will increase. On the contrary, the value of the factor level. The narrower the range, the less significant the factor. This is why d fails the significance test in the available range of values.

To sum up, the diameter of the cooling channel, the distance between the centers of adjacent cooling channels, and the distance from the centerline of the cooling channel to the cavity are all important variables in the design of the conformal cooling channel, and are important factors affecting product cooling.

In order to judge the degree of influence of each factor on the test indicators, the test results are now analyzed by range as shown in Table 16, according to the size of the range R , there are $R_s > R_l > R_d$, then for the test index. The degree of influence is $s > l > d$, the distance from the centerline of the cooling channel to the cavity has the most significant influence, followed by the distance between the centers of adjacent cooling channels, and finally the diameter of the cooling channel.

Table 16 Test result range analysis table

| Test No. | d | l | $the s$ | empty column | $Y_{\Delta T}$ |
|----------|-----|-----|---------|--------------|----------------|
| 1 | 1 | 1 | 1 | 1 | 63.143 |
| 2 | 1 | 2 | 2 | 2 | 68.041 |
| 3 | 1 | 3 | 3 | 3 | 72.793 |
| 4 | 2 | 1 | 2 | 3 | 66.601 |
| 5 | 2 | 2 | 3 | 1 | 71.34 |
| 6 | 2 | 3 | 1 | 2 | 64.798 |
| 7 | 3 | 1 | 3 | 2 | 70.298 |
| 8 | 3 | 2 | 1 | 3 | 63.651 |

| 9 | 3 | 3 | 2 | 1 | 68.167 |
|-------|-------|-------|-------|-------|--------|
| K_1 | 67.99 | 66.68 | 63.86 | 67.55 | |
| K_2 | 67.58 | 67.68 | 67.60 | 67.71 | 608.83 |
| K_3 | 67.37 | 68.59 | 71.48 | 67.68 | |
| R | 0.62 | 1.91 | 7.61 | 0.16 | |

5.3 Optimal experimental design and analysis of results

The purpose of the optimal design of the conformal cooling channels is to obtain a uniform temperature distribution on the product surface and minimize the cooling time. In order to study the optimal cooling effect of the product when the design parameters of the conformal cooling channel are selected. By studying the influence of different design variables on the cooling effect, the quantitative relationship between the indicators and the design variables is investigated to guide the mold designer in the design of the conformal cooling channels.

The test adopts the Box-Behnken test method (RSM) to conduct response surface analysis, establish the corresponding predictive regression model and carry out analysis of variance and use the residual probability map for reliability verification, get the quadratic equation of the interaction term and the square term, analyze the main effect and interaction effect of each factor, and finally find the optimal value within a certain range. is then combined with the NSGA-II algorithm for multi-objective optimization to obtain the best factor level combination value.

5.3.1 Determination of optimization variables and response indicators

In daily production, the wall thickness of common injection molded parts varies in the range of 0-6 mm. Plastic parts with different shapes,

sizes and wall thicknesses need to be designed with different shapes. Cooling channel design configuration, that is, the diameter of the cooling channel (circular cooling channel), the distance between the centers of adjacent cooling channels, the distance from the centerline of the cooling channel to the cavity, etc., so as to ensure the cooling of the product. The effect is optimal. Considering the impact of wall thickness on product cooling, this experiment investigates the effect of conformal water cooling on three products of the same shape and size with different wall thickness. Experimental design divided into 3 groups: DOE-1, DOE-2 and DOE-3, where DOE-1 to DOE-3 respectively, the wall thicknesses of curved sheet plastic parts are 1.5mm, 3.5mm and 6mm. Protocol under. After determining the design variables, it is necessary to determine the cross-sectional geometry and arrangement type of the cooling channel. Z-shaped circular cross-section conformal cooling channels arranged in series can provide effective thermal performance for injection molds, therefore, all the above design cases use circular cross-section conduct optimization tests on the conformal cooling channels arranged in series.

The product and cooling channel model in the test are same, and the test takes cooling time y_t and product cooling uniformity $y_{\Delta t}$ as response indicators, the cooling channel diameter d , the distance between adjacent cooling channel l , and the distance s from the centerline of the cooling channel to the cavity are used as optimization variables. Three levels are taken for each variable, and the value range of the level is determined from the experience of the mold designer and the existing literature. Table 17 shows the value range of the cooling channel design variables with different wall thicknesses, where y_t is measured by the average time from the start of injection to reaching the ejection temperature, $y_{\Delta t}$ is measured by the standard deviation of the temperature distribution of the plastic part at the moment of reaching the

ejection temperature, the smaller the response indices y_t and $y_{\Delta t}$, the better the cooling effect of the conformal cooling channels.

Table 17 Value ranges of cooling channel design variables with different wall thicknesses

| Wall thickness/mm | d /mm | l /mm | s /mm |
|-------------------|---------|---------|---------|
| 1.5 | 4-8 | 12-24 | 8-16 |
| 3.5 | 8-12 | 16-36 | 12-24 |
| 5.5 | 12-14 | 24-42 | 18-28 |

Table 18 DOE-1, DOE-2, DOE-3 optimization specification

| | DOE-1 | DOE-2 | DOE-3 |
|--------------------|--|--|--|
| Objective Function | 1. Minimum cooling time y_t | 1. Minimum cooling time y_t | 1. Minimum cooling time y_t |
| | 2. Minimum cooling uniformity $y_{\Delta t}$ | 2. Minimum cooling uniformity $y_{\Delta t}$ | 2. Minimum cooling uniformity $y_{\Delta t}$ |
| Design Variable | Channel diameter d | Channel diameter d | Channel diameter d |
| | Distance between adjacent channels l | Distance between adjacent channels l | Distance between adjacent channels l |
| | Distance from cooling channel centerline to cavity s | Distance from cooling channel centerline to cavity s | Distance from cooling channel centerline to cavity s |
| B.C. | $\delta \leq 2\text{mm}$ | $2\text{mm} < \delta \leq 4\text{mm}$ | $4\text{mm} < \delta < 6\text{mm}$ |
| | $4\text{mm} < d < 8\text{mm}$ | $8\text{mm} < d < 12\text{mm}$ | $12\text{mm} < d < 14\text{mm}$ |
| | $12\text{mm} < l < 24\text{mm}$ | $16\text{mm} < l < 36\text{mm}$ | $24\text{mm} < l < 42\text{mm}$ |
| | $8\text{mm} < s < 16\text{mm}$ | $12\text{mm} < s < 24\text{mm}$ | $18\text{mm} < s < 28\text{mm}$ |

5.3.2 Response Surface Design of Experiments

According to the introduction of the previous optimization test method, Box-Behnken is a three-level The second-order experimental design method, which is suitable for optimization experiments with 2~5 factors, can be used to predict nonlinear relationships between variables and response values. When the factors are the same, because there is no axial point, BBD The number of experimental designs is economical, and the level value of the optimal combination obtained by the optimization solution will not exceed the highest value The range is, and it has relatively accurate prediction accuracy and high operating efficiency. Considering the practical problems of manufacturing (such as mold strength), the values of optimization variables must be limited within a given range, so BBD methods are more suitable for this optimization analyze.

According to the experimental principle of RSM, first code the levels of each factor with (-1,0,1), and design the table arrangement is centered on 0, -1 and 1 represent the minimum level and high level value of the factor respectively. The specific values after coding the corresponding factor levels in the three groups of experiments are shown in Table 19.

Table 19 DOE-1 DOE-2 DOE-3 values

| DOE-1 | | | | DOE-2 | | | | DOE-3 | | | |
|-------|----------|----------|----------|-------|----------|----------|----------|-------|----------|----------|----------|
| Level | <i>d</i> | <i>l</i> | <i>s</i> | Level | <i>d</i> | <i>l</i> | <i>s</i> | Level | <i>d</i> | <i>l</i> | <i>s</i> |
| -1 | 4 | 12 | 8 | -1 | 8 | 16 | 12 | -1 | 12 | 24 | 18 |
| 0 | 6 | 18 | 12 | 0 | 10 | 26 | 18 | 0 | 13 | 33 | 23 |
| 1 | 8 | 24 | 16 | 1 | 12 | 36 | 24 | 1 | 14 | 42 | 28 |

The cooling effect of the conformal cooling water channel is related to the diameter of the water channel, the center distance between adjacent

water channels, and the distance between the center line of the water channel and the cavity. The distance of is non-linear, so we directly carry out the second-order response surface combination design, that is, select test points with different characteristics in the coding space to form a test plan. Use software to conduct Box-Behnken experimental design, the generated response surface experimental design is shown in Table 20.

Table 20 Box-Behnken Experimental Design Table

| Experimental point | d | l | s |
|--------------------|-----|-----|-----|
| 1 | -1 | -1 | 0 |
| 2 | 1 | -1 | 0 |
| 3 | -1 | 1 | 0 |
| 4 | 1 | 1 | 0 |
| 5 | -1 | 0 | -1 |
| 6 | 1 | 0 | -1 |
| 7 | -1 | 0 | 1 |
| 8 | 1 | 0 | 1 |
| 9 | 0 | -1 | -1 |
| 10 | 0 | 1 | -1 |
| 11 | 0 | -1 | 1 |
| 12 | 0 | 1 | 1 |
| 13 | 0 | 0 | 0 |
| 14 | 0 | 0 | 0 |
| 15 | 0 | 0 | 0 |

The design needs to carry out 15 groups of experiments, among which the former 12 Group test points are factorial points, followed by 3 groups are repeated cubic center experimental points, the purpose is to estimate the experimental error. Input each factor and level value in turn into software to generate DOE-1 to DOE-3 specific test program arrangement.

Table 21 DOE-1, DOE-2, DOE-3 test plan

| DOE-1 | DOE-2 | DOE-3 |
|-------|-------|-------|
|-------|-------|-------|

| Test No. | d (mm) | l (mm) | s (mm) | Test No. | d (mm) | l (mm) | s (mm) | Test No. | d (mm) | l (mm) | s (mm) |
|----------|-------------|-------------|-------------|----------|-------------|-------------|-------------|----------|-------------|-------------|-------------|
| 1.1 | 4 | 12 | 12 | 2.1 | 8 | 16 | 18 | 3.1 | 12 | 24 | 23 |
| 1.2 | 8 | 12 | 12 | 2.2 | 12 | 16 | 18 | 3.2 | 14 | 24 | 23 |
| 1.3 | 4 | 24 | 12 | 2.3 | 8 | 36 | 18 | 3.3 | 12 | 42 | 23 |
| 1.4 | 8 | 24 | 12 | 2.4 | 12 | 36 | 18 | 3.4 | 14 | 42 | 23 |
| 1.5 | 4 | 18 | 8 | 2.5 | 8 | 26 | 12 | 3.5 | 12 | 33 | 18 |
| 1.6 | 8 | 18 | 8 | 2.6 | 12 | 26 | 12 | 3.6 | 14 | 33 | 18 |
| 1.7 | 4 | 18 | 16 | 2.7 | 8 | 26 | 24 | 3.7 | 12 | 33 | 28 |
| 1.8 | 8 | 18 | 16 | 2.8 | 12 | 26 | 24 | 3.8 | 14 | 33 | 28 |
| 1.9 | 6 | 12 | 8 | 2.9 | 10 | 16 | 12 | 3.9 | 13 | 24 | 18 |
| 1.10 | 6 | 24 | 8 | 2.10 | 10 | 36 | 12 | 3.10 | 13 | 42 | 18 |
| 1.11 | 6 | 12 | 16 | 2.11 | 10 | 16 | 24 | 3.11 | 13 | 24 | 28 |
| 1.12 | 6 | 24 | 16 | 2.12 | 10 | 36 | 24 | 3.12 | 13 | 42 | 28 |
| 1.13 | 6 | 18 | 12 | 2.13 | 10 | 26 | 18 | 3.13 | 13 | 33 | 23 |
| 1.14 | 6 | 18 | 12 | 2.14 | 10 | 26 | 18 | 3.14 | 13 | 33 | 23 |
| 1.15 | 6 | 18 | 12 | 2.15 | 10 | 26 | 18 | 3.15 | 13 | 33 | 23 |

UG software is used to model the test points of DOE-1, DOE-2 and DOE-3 in sequence, and then the model of the test points is imported into Moldflow for simulation, and the test results of DOE-1 to DOE-3 are shown in Table 22.

Table 22 DOE-1, DOE-2, DOE-3 test result

| DOE-1 | | | DOE-2 | | | DOE-3 | | |
|----------|-------------------|-------------------|----------|----------|-------------------|----------|----------|-------------------|
| Test No. | $y_{\Delta T}(s)$ | $y_{\Delta t}(s)$ | Test No. | $y_t(s)$ | $y_{\Delta T}(s)$ | Test No. | $y_t(s)$ | $y_{\Delta T}(s)$ |
| 1.1 | 6.272 | 1.815 | 2.1 | 18.133 | 1.040 | 3.1 | 46.780 | 2.377 |
| 1.2 | 6.252 | 1.724 | 2.2 | 18.297 | 1.092 | 3.2 | 46.560 | 2.397 |
| 1.3 | 6.639 | 2.286 | 2.3 | 19.000 | 1.585 | 3.3 | 51.548 | 2.793 |
| 1.4 | 6.552 | 2.155 | 2.4 | 19.061 | 1.594 | 3.4 | 51.448 | 2.820 |
| 1.5 | 6.039 | 1.515 | 2.5 | 17.555 | 0.752 | 3.5 | 44.091 | 2.067 |
| 1.6 | 5.983 | 1.370 | 2.6 | 17.641 | 0.740 | 3.6 | 44.362 | 2.068 |
| 1.7 | 6.912 | 2.612 | 2.7 | 19.647 | 1.917 | 3.7 | 53.845 | 2.966 |

| | | | | | | | | |
|------|-------|-------|------|--------|-------|------|--------|-------|
| 1.8 | 6.869 | 2.548 | 2.8 | 19.660 | 1.892 | 3.8 | 53.400 | 2.961 |
| 1.9 | 5.868 | 1.089 | 2.9 | 17.199 | 0.436 | 3.9 | 42.177 | 1.854 |
| 1.10 | 6.151 | 1.637 | 2.10 | 17.969 | 1.028 | 3.10 | 46.465 | 2.392 |
| 1.11 | 6.690 | 2.337 | 2.11 | 19.209 | 1.680 | 3.11 | 51.971 | 2.806 |
| 1.12 | 7.014 | 2.698 | 2.12 | 19.994 | 2.104 | 3.12 | 55.687 | 3.145 |
| 1.13 | 6.429 | 2.076 | 2.13 | 18.611 | 1.359 | 3.13 | 48.740 | 2.590 |
| 1.14 | 6.433 | 2.077 | 2.14 | 18.660 | 1.381 | 3.14 | 48.595 | 2.521 |
| 1.15 | 6.495 | 2.056 | 2.15 | 18.599 | 1.378 | 3.15 | 48.611 | 2.566 |

whether the above functional model can well reflect the functional relationship between the optimization variable and the response index, or whether it can be used as a meaningful second-order approximation model, it is necessary to perform residual and variance analysis on the model to test the significance test and regression of the equation. The significance of the coefficient is used to measure the accuracy of model fitting and the excellence of the model.

Hypothesis H_0 : The regression equation is not out of fit, and the model fit is good; Hypothesis H_{02} : The relationship between the variable and the response value. There is no linear relationship between; Assumptions H_{03} : There is no curvilinear relationship between variables and response values; Assumptions H_{04} : Interaction term has no effect on the response value.

It can be seen from Table 23 that the lack-of-fit test P values of the two response surface models are 0.840 and 0.776, both of which are greater than 0.05, reject the null hypothesis, indicating that the above two regression equations are not out of fit, and the model fits well. Because the model-adjusted regression goodness of fit is 0.9936 and 0.9996 is very close to 1, so it can be considered that the above regression equations on cooling time and product cooling uniformity have very high fitting accuracy as a whole.

Table 23 DOE-1 ANOVA Table (cooling time)

| Source | df | SS | MS | F-Value | P-Value | Significance |
|------------------------|----|---------|---------|---------|---------|--------------|
| Model | 9 | 1.69418 | 0.18824 | 242.51 | 0.000 | ** |
| Linear | 3 | 1.69083 | 0.56361 | 726.08 | 0.000 | ** |
| <i>d</i> | 1 | 0.00530 | 0.00530 | 6.83 | 0.047 | * |
| <i>l</i> | 1 | 0.20288 | 0.20288 | 261.37 | 0.000 | ** |
| <i>s</i> | 1 | 1.48264 | 1.48264 | 1910.05 | 0.000 | ** |
| Square | 3 | 0.00177 | 0.00059 | 0.76 | 0.563 | |
| <i>d * d</i> | 1 | 0.00001 | 0.00001 | 0.02 | 0.906 | |
| <i>l * l</i> | 1 | 0.00175 | 0.00175 | 2.26 | 0.193 | |
| <i>s * s</i> | 1 | 0.00000 | 0.00000 | 0.00 | 0.989 | |
| two-way interaction | 3 | 0.00158 | 0.00053 | 0.68 | 0.601 | |
| <i>d * l</i> | 1 | 0.00112 | 0.00112 | 1.45 | 0.283 | |
| <i>d * s</i> | 1 | 0.00004 | 0.00004 | 0.05 | 0.825 | |
| <i>l * s</i> | 1 | 0.00042 | 0.00042 | 0.54 | 0.495 | |
| Error | 5 | 0.00388 | 0.00078 | | | |
| Lack-of-fit | 3 | 0.00114 | 0.00038 | 0.28 | 0.840 | |
| Pure error | 2 | 0.00274 | 0.00137 | | | |
| Total | 14 | 1.69806 | | | | |

Note: $R^2 = 99.77\%$, R^2 (adj) = 99.36%.

Table 24 DOE-1 ANOVA table (uniformity of part temperature distribution)

| Source | df | SS | MS | F | P | significance |
|--------------|----|---------|---------|----------|-------|--------------|
| Model | 9 | 3.10019 | 0.34447 | 3697.96 | 0.000 | ** |
| Linear | 3 | 3.05982 | 1.01994 | 10949.43 | 0.000 | ** |
| <i>d</i> | 1 | 0.02322 | 0.02322 | 249.28 | 0.000 | ** |
| <i>l</i> | 1 | 0.40997 | 0.40997 | 4401.13 | 0.000 | ** |
| <i>s</i> | 1 | 2.62663 | 2.62663 | 28197.87 | 0.000 | ** |
| Square | 3 | 0.02959 | 0.00986 | 105.87 | 0.000 | ** |
| <i>d * d</i> | 1 | 0.00001 | 0.00001 | 0.16 | 0.707 | |
| <i>l * l</i> | 1 | 0.01968 | 0.01968 | 211.23 | 0.000 | ** |

| | | | | | | |
|------------------------|----|---------|---------|--------|-------|----|
| $s*s$ | 1 | 0.01189 | 0.01189 | 127.66 | 0.000 | ** |
| two-way interaction | 3 | 0.01078 | 0.00359 | 38.58 | 0.001 | ** |
| $d * l$ | 1 | 0.00040 | 0.00040 | 4.29 | 0.093 | |
| $d * s$ | 1 | 0.00164 | 0.00164 | 17.61 | 0.009 | ** |
| $l * s$ | 1 | 0.00874 | 0.00874 | 93.85 | 0.000 | ** |
| Error | 5 | 0.00047 | 0.00009 | | | |
| Lack-of-fit | 3 | 0.00017 | 0.00006 | 0.39 | 0.776 | |
| Pure error | 2 | 0.00029 | 0.00015 | | | |
| Total | 14 | 3.10065 | | | | |

It can be seen from Table 23 that the overall test of the linear relationship item is $P < 0.05$, and the initial hypothesis H_{02} is not established, indicating that in this model, the overall linear relationship is statistically significant. Since the P value of the primary item is also less than 0.05, it can be seen that the main effect has an impact on the response y_t . Both are significant. Since the P-values of the quadratic and interaction F-tests are greater than 0.05, the hypotheses H_{03} and H_{04} are accepted, it means quadratic and interaction terms have little to no effect on the response y_t . It can be seen from Table 24 that the overall test P values of the linear relationship item, the square item and the interaction item are all less than 0.05, then reject the null hypothesis H_{02} , H_{03} and H_{04} , it can be known that the overall main effect, quadratic term and interaction term are statistically significant significance d^2 for the quadratic term and $d \cdot l$ for the interaction term greater than 0.05 multiple responses $y_{\Delta T}$ have no effect, other terms have no effect on responses $y_{\Delta T}$.

In summary,

$$y_t = 4.521 - 0.0128d + 0.0516l + 0.0972s + 0.00045d^2 - 0.000605l^2 + 0.000013s^2 - 0.00140d \cdot l + 0.00041d \cdot s + 0.000427l \cdot s \quad (5-7)$$

$$y_{\Delta T} = -1.677 - 0.0368d + 0.13894l + 0.24800s - 0.00046d^2 - 0.002023l^2 - 0.003536s^2 - 0.00833d \cdot l + 0.002531d \cdot s - 0.001948l \cdot s \quad (5-8)$$

The regression equation is obtained by fitting the DOE-1 response surface through curve fitting.

Under normal circumstances, for the partial regression coefficients that do not pass the significance test, it is generally necessary to remove the ineffective items from the model and then re-model. Given that the adjusted in the regression equation for y_t in the above equation is 0.9936, the predicted R is 0.9856, both are very close to 1, so it can be considered that the response model of y_t is very stable, the fitting accuracy is sufficient, there is no need to Model remodeling. For the regression equation of $y_{\Delta T}$, the adjusted R is 0.9996, and the predicted R is 0.9989, which is also very close to 1, it confirms that the equations are available and very reliable. Then conducting residual analysis on the y_t and $y_{\Delta T}$ regression equations of DOE-1. In the normal probability plot, the experimental points are evenly distributed around the straight line, indicating that the errors of the experimental points follow a normal distribution. In the standardized residual plot, there is no visible pattern or systematic distribution of points, suggesting homoscedasticity and a good fit of the model.

In the normal probability chart, the test points all fall near the straight line, it can be seen that the test point errors obey the normal distribution. In the standardized residual graph, there is no regular point distribution such as horn shape, indicating that the variance is homogeneous and the model fits well.

(2) DOE-2 test of the model

1. Model checking

DOE-2 test data ANOVA table is shown in Table 25 and Table 26.

Table 25 DOE-2 ANOVA table (cooling time)

| source | df | SS | MS | F | P | significance |
|------------------------|----|---------|---------|---------|-------|--------------|
| Model | 9 | 9.58354 | 1.06484 | 965.02 | 0.000 | ** |
| linear | 3 | 9.57661 | 3.19220 | 2892.97 | 0.000 | ** |
| <i>d</i> | 1 | 0.01312 | 0.01312 | 11.89 | 0.018 | * |
| <i>l</i> | 1 | 1.26882 | 1.26882 | 1149.89 | 0.000 | ** |
| <i>the s</i> | 1 | 8.29466 | 8.29466 | 7517.14 | 0.000 | ** |
| square | 3 | 0.00288 | 0.00096 | 0.87 | 0.514 | |
| <i>d * d</i> | 1 | 0.00097 | 0.00097 | 0.88 | 0.391 | |
| <i>l * l</i> | 1 | 0.00104 | 0.00104 | 0.94 | 0.376 | |
| <i>s*s</i> | 1 | 0.00070 | 0.00070 | 0.64 | 0.461 | |
| two-factor interaction | 3 | 0.00404 | 0.00135 | 1.22 | 0.393 | |
| <i>d * l</i> | 1 | 0.00265 | 0.00265 | 2.40 | 0.182 | |
| <i>d * s</i> | 1 | 0.00133 | 0.00133 | 1.21 | 0.322 | |
| <i>l * s</i> | 1 | 0.00006 | 0.00006 | 0.05 | 0.830 | |
| error | 5 | 0.00552 | 0.00110 | | | |
| lack of fit | 3 | 0.00343 | 0.00114 | 1.09 | 0.510 | |
| pure error | 2 | 0.00209 | 0.00104 | | | |
| total | 14 | 9.58905 | | | | |

Table 26 DOE-2 ANOVA table (uniformity of part temperature distribution)

| source | df | SS | MS | F | P | significance |
|--------------|----|---------|---------|---------|-------|--------------|
| Model | 9 | 3.23417 | 0.35935 | 1118.49 | 0.000 | ** |
| linear | 3 | 3.21979 | 1.07326 | 3340.55 | 0.000 | ** |
| <i>d</i> | 1 | 0.00007 | 0.00007 | 0.22 | 0.656 | |
| <i>l</i> | 1 | 0.53200 | 0.53200 | 1655.85 | 0.000 | ** |
| <i>the s</i> | 1 | 2.68772 | 2.68772 | 8365.58 | 0.000 | ** |
| square | 3 | 0.00682 | 0.00227 | 7.07 | 0.030 | * |
| <i>d * d</i> | 1 | 0.00093 | 0.00093 | 2.88 | 0.150 | |
| <i>l * l</i> | 1 | 0.00312 | 0.00312 | 9.72 | 0.026 | * |

| | | | | | | |
|------------------------|----|---------|---------|-------|-------|----|
| $s*s$ | 1 | 0.00368 | 0.00368 | 11.46 | 0.020 | * |
| two-factor interaction | 3 | 0.00756 | 0.00252 | 7.84 | 0.024 | * |
| $d * l$ | 1 | 0.00046 | 0.00046 | 1.44 | 0.284 | |
| $d * s$ | 1 | 0.00004 | 0.00004 | 0.13 | 0.732 | |
| $l * s$ | 1 | 0.00706 | 0.00706 | 21.96 | 0.005 | ** |
| error | 5 | 0.00161 | 0.00032 | | | |
| lack of fit | 3 | 0.00132 | 0.00044 | 3.10 | 0.254 | |
| pure error | 2 | 0.00028 | 0.00014 | | | |
| total | 14 | 3.23577 | | | | |

The P values of the lack of fit test of the two response surface models of DOE-2 are 0.510 and 0.254 respectively, both are greater than 0.05, so the null hypothesis is rejected H_{01} , it can be considered that the above two regression equations fit well. Since the model-adjusted regression fit R^2 is 0.9984 and 0.9986 respectively, both of which are very close to 1, it can be considered that the above cooling time and product cooling are uniform the regression equations of degree have very high fitting accuracy.

It can be seen from Table 25 that the overall test of the linear relationship item is $P < 0.05$, and the initial hypothesis H_{02} is rejected, indicating that in this model, the overall linear relationship is statistically significant. Since the P value of the primary item is also less than 0.05, it can be seen that the main effect has an impact on the response y_t . Both are significant. Since the P-values of the quadratic and interaction F-tests are greater than 0.05, the hypotheses H_{03} and H_{04} are accepted, it means quadratic and interaction terms have little to no effect on the response y_t . It can be seen from Table 26 that the overall test P values of the linear relationship item, the square item and the interaction item are all less than 0.05, then reject the null hypothesis H_{02} , H_{03} and H_{04} , it can be known that the overall main effect, quadratic term and interaction

term are statistically significant significance d^2 for the quadratic term and $d \cdot l$ for the interaction term greater than 0.05 multiple responses $y_{\Delta T}$ have no effect, other terms have no effect on responses $y_{\Delta T}$.

In summary,

$$y_t = 13.919 + 0.0001d + 0.0603l + 0.1971s - 0.00405d^2 - 0.000168l^2 - 0.000383s^2 - 0.001288d \cdot l - 0.00152d \cdot s + 0.000063l \cdot s \quad (5-9)$$

$$y_{\Delta T} = -2.444 + 0.0995d + 0.05889l + 0.1491s - 0.00396d^2 - 0.000291l^2 - 0.000877s^2 - 0.000537d \cdot l - 0.000271d \cdot s - 0.000700l \cdot s \quad (5-10)$$

Adjusted R^2 and predicted R^2 in the regression equation due to y_T are 0.9984 and 0.9938, respectively, $y_{\Delta T}$ in the regression equation adjusted R^2 and the predicted R^2 are 0.9984 and 0.9938, respectively, both are very close to 1, the equation has sufficient fitting accuracy and is reliable for predicting the response index.

Since the assumption of variance analysis requires the data to obey the normal distribution, the regression equation of y_T and $y_{\Delta T}$ is used for residual diagnosis. The test points in the normal probability chart all fall near the straight line, and it can be seen that the test point errors obey the normal distribution. In the standardized residual graph, there is no regular point distribution such as horn shape, indicating that the variance is homogeneous and the model fits well.

3) DOE-3 test of the model

DOE-3 test data ANOVA table is shown in Table 27 and Table 28.

Table 27 DOE-3 ANOVA table (cooling time)

| source | df | SS | MS | f | P | Significance |
|---------|----|---------|---------|---------|-------|--------------|
| Model | 9 | 218.318 | 24.258 | 334.39 | 0.000 | ** |
| linear | 3 | 217.696 | 72.565 | 1000.31 | 0.000 | ** |
| d | 1 | 0.031 | 0.031 | 0.42 | 0.545 | |
| l | 1 | 38.984 | 38.984 | 537.40 | 0.000 | ** |
| $the s$ | 1 | 178.681 | 178.681 | 2463.10 | 0.000 | ** |
| square | 3 | 0.409 | 0.136 | 1.88 | 0.251 | |

| | | | | | |
|------------------------|----|---------|-------|-------|-------|
| <i>d * d</i> | 1 | 0.075 | 0.075 | 1.03 | 0.356 |
| <i>l * l</i> | 1 | 0.317 | 0.317 | 4.37 | 0.091 |
| <i>s * s</i> | 1 | 0.066 | 0.066 | 0.91 | 0.385 |
| two-factor interaction | 3 | 0.214 | 0.071 | 0.98 | 0.472 |
| <i>d * l</i> | 1 | 0.004 | 0.004 | 0.05 | 0.833 |
| <i>d * s</i> | 1 | 0.128 | 0.128 | 1.77 | 0.241 |
| <i>l * s</i> | 1 | 0.082 | 0.082 | 1.13 | 0.337 |
| error | 5 | 0.363 | 0.073 | | |
| Lack of fit | 3 | 0.350 | 0.117 | 18.46 | 0.052 |
| pure error | 2 | 0.013 | 0.006 | | |
| total | 14 | 218.681 | | | |

Note: $R^2 = 99.83$, R^2 (adjusted)=99.54%

Table 28 DOE-3 ANOVA table (uniformity of part temperature distribution)

| source | df | SS | MS | f | P | Significance |
|------------------------|----|---------|---------|---------|-------|--------------|
| Model | 9 | 1.92025 | 0.21336 | 273.14 | 0.000 | ** |
| linear | 3 | 1.89694 | 0.63231 | 809.46 | 0.000 | ** |
| <i>d</i> | 1 | 0.00023 | 0.00023 | 0.30 | 0.610 | |
| <i>l</i> | 1 | 0.36808 | 0.36808 | 471.21 | 0.000 | ** |
| <i>the s</i> | 1 | 1.52863 | 1.52863 | 1956.89 | 0.000 | ** |
| square | 3 | 0.01339 | 0.00446 | 5.72 | 0.045 | * |
| <i>d * d</i> | 1 | 0.00001 | 0.00001 | 0.02 | 0.896 | |
| <i>l * l</i> | 1 | 0.00472 | 0.00472 | 6.04 | 0.057 | |
| <i>s * s</i> | 1 | 0.00764 | 0.00764 | 9.79 | 0.026 | * |
| two-factor interaction | 3 | 0.00992 | 0.00331 | 4.23 | 0.077 | |
| <i>d * l</i> | 1 | 0.00001 | 0.00001 | 0.02 | 0.905 | |
| <i>d * s</i> | 1 | 0.00001 | 0.00001 | 0.01 | 0.919 | |
| <i>l * s</i> | 1 | 0.00990 | 0.00990 | 12.67 | 0.016 | * |
| error | 5 | 0.00391 | 0.00078 | | | |
| Lack of fit | 3 | 0.00145 | 0.00048 | 0.39 | 0.773 | |
| pure error | 2 | 0.00245 | 0.00123 | | | |
| total | 14 | 1.92416 | | | | |

Note: $R^2 = 99.80$, R^2 (adjusted)=99.43

According to Table 27 and Table 28, the p-values for lack of fit tests of

the y_T and $y_{\Delta T}$ models are both greater than 0.05, indicating that both models fit well and do not exhibit lack of fit. Additionally, the adjusted R-squared values for the two models are 0.9954 and 0.9943, respectively, which are very close to 1, indicating a high level of fitting accuracy for both regression equations.

From Table 27, it can be observed that the overall test p-value for the linear relationship is less than 0.05, and the p-values for the main effects l and s are also less than 0.05, indicating a significant impact on the response y_T . However, the p-values for the quadratic terms and interaction terms are greater than 0.05, suggesting that they have little to no effect on the response y_T and can be ignored. Furthermore, from Table 28, the overall test p-values for the linear and quadratic terms are both less than 0.05, indicating that the main effects and quadratic terms are statistically significant for the overall model. Among them, the main effects l , s , and the quadratic terms s^2 , as well as the interaction term $l \cdot s$, have p-values less than 0.05, indicating their importance in the $y_{\Delta T}$ response model.

In summary, the response model for DOE-3 is

$$y_t = 38.8 - 3.05d + 0.036l + 1.270s + 0.142d^2 + 0.00362l^2 + 0.00534s^2 + 0.0033d \cdot l - 0.0358d \cdot s - 0.00318l \cdot s \quad (5-11)$$

$$y_{\Delta t} = -1.30 - 0.046d + 0.0176l + 0.2115s + 0.0020d^2 + 0.000441l^2 - 0.001820s^2 + 0.00019d \cdot l - 0.00030d \cdot s - 0.001106l \cdot s \quad (5-12)$$

After doing analysis of variance, significance test and residual analysis on the above models, the response model of $y_{\Delta T}$ is stable, fitting Accurate enough. The test points in the normal probability chart all fall near the straight line, and it can be seen that the errors of the test points obey the normal distribution. In the standardized residual graph, there is no regular point distribution such as horn shape, which again shows that the variance is homogeneous and the model fits well.

In DOE-1 and DOE-2, the variables d , l , s have a significant impact on the response index y_T , while in DOE-3, only the variables l and s have a significant impact on the indicators, and d has no impact on the response indicators y_T . When the wall thickness of the plastic part is 1.5mm and 3.5mm, the three design variables of the cooling channel diameter d , the distance l between adjacent cooling channels and the distance s from the cooling channel to the cavity all have a significant impact on the cooling time, the degree of influence. And when the wall thickness of the plastic part increases to 6mm, the effect of the diameter of the water channel on the cooling time can gradually be ignored. This is because as the wall thickness increases, the heat brought into the cavity by the plastic melt increases. Due to the large wall thickness, the heat inside the plastic part accumulates and is difficult to release in a short period of time. In the smaller value range 12~14 mm, the change of the diameter of the cooling channel has little effect on the index. Therefore, in the conformal cooling channel design process, when the minimum cooling time is the optimization goal, when the product wall thickness is less than 4mm, the optimized design variables include the channel diameter, Distance between the adjacent channels and the distance from the cooling channel to the cavity; when the product wall thickness is greater than 4mm, the diameter of the cooling channel can be constrained, and the design variables should focus on optimizing the adjacent cooling channel Pitch and distance from cooling channel to cavity.

When the minimum cooling time is the optimization objective, for product wall thicknesses less than 2mm, the optimized design variables should include water channel diameter, distance between the adjacent channels, and distance from the water channel to the cavity. However, for product wall thicknesses greater than 2mm, the water channel diameter only needs to fall within the corresponding constrained range, while the

optimization design of the water channel mainly focuses on the design variables of distance between the adjacent channels and distance from the water channel to the cavity.

5.4 Multi-objective optimization

From the results of response surface analysis, it can be seen that the design parameters of the cooling channels have a significant impact on the cooling time and temperature distribution uniformity of the product. In engineering applications, shortening the molding cycle as much as possible and improving product molding quality are the tireless pursuit goals of enterprises. Therefore, the design of the conformal cooling channels must be able to shorten the cooling time of the product, and at the same time improve the temperature distribution uniformity of the product as much as possible, which requires simultaneous design optimization of the two optimization objectives.

This chapter optimizes the objective function using the NSGA-II algorithm based on Pareto optimal frontier solutions. Cooling time *Obj1* and product cooling uniformity obtained in response surface model *Obj2* as the optimization objective, taking the cooling channel diameter, the distance between adjacent the cooling channel to the distance of the cavity is the decision variable to solve the two objectives.

The optimization model of DOE-1-DOE-3 is as follows:

(1) DOE-1

Objective function 1:

$$\text{Min } Obj1 = 4.521 - 0.0128d + 0.0516l + 0.0972s + 0.00045d^2 - 0.000605l^2 + 0.000013s^2 - 0.00140d \cdot l + 0.00041d \cdot s + 0.000427l \cdot s \quad (5-13)$$

Objective function 2:

$$\begin{aligned} \text{Min } Obj1 = & -1.677 - 0.0368d + 0.13894l + 0.24800s - 0.00046d^2 \\ & - 0.002023l^2 - 0.003536s^2 - 0.00833d \cdot l + 0.002531d \cdot s \\ & - 0.001948l \cdot s \end{aligned} \quad (5-14)$$

B.C.:

$$\text{s.t } \begin{cases} 4 < d \leq 8 \\ 8 < l \leq 24 \\ 6 < s \leq 16 \\ l - d \geq 4 \\ s - \frac{d}{2} \geq 4 \end{cases} \quad (5-15)$$

(2)DOE-2

Objective function 1:

$$\begin{aligned} \text{Min } Obj1 = & 13.919 + 0.0001d + 0.0603l + 0.1971s - 0.00405d^2 - 0.000168l^2 \\ & - 0.000383s^2 - 0.001288d \cdot l - 0.00152d \cdot s + 0.000063l \cdot s \end{aligned} \quad (5-16)$$

Objective function 2:

$$\begin{aligned} \text{Min } Obj2 = & -2.444 + 0.0995d + 0.05889l + 0.1491s - 0.00396d^2 - \\ & 0.000291l^2 - 0.000877s^2 - 0.000537d \cdot l - 0.000271d \cdot s - 0.000700l \cdot s \end{aligned} \quad (5-17)$$

B.C.:

$$\text{s.t } \begin{cases} 8 \leq d \leq 12 \\ 16 \leq l \leq 36 \\ 12 \leq s \leq 24 \\ l - d \geq 4 \\ s - \frac{d}{2} \geq 4 \end{cases} \quad (5-18)$$

(3)DOE-3

Objective function 1:

$$\begin{aligned} \text{Min } Obj1 = & 38.8 - 3.05d + 0.036l + 1.270s + 0.142d^2 + 0.00362l^2 + \\ & 0.00534s^2 + 0.0033d \cdot l - 0.0358d \cdot s - 0.00318l \cdot s \end{aligned} \quad (5-19)$$

Objective function 2:

$$\begin{aligned} \text{Min } Obj2 = & -1.30 - 0.046d + 0.0176l + 0.2115s + 0.0020d^2 + 0.000441l^2 - \\ & 0.001820s^2 + 0.00019d \cdot l - 0.00030d \cdot s - 0.001106l \cdot s \end{aligned} \quad (5-20)$$

B.C.:

$$\text{s.t.} \begin{cases} 12 \leq d \leq 14 \\ 24 \leq l \leq 42 \\ 18 \leq s \leq 28 \\ l - d \geq 4 \\ s - \frac{d}{2} \geq 4 \end{cases} \quad (5-21)$$

In practical production, different products will have different requirements. When the product requires high dimensional accuracy, in Pareto frontier solution set, you should choose *Obj1* is larger and *Obj2* is smaller, as shown in Fig. 17, take the corresponding decision variable value here as a reference for conformal cooling channel design. On the contrary, when the precision of the product is not high, you should choose the value at B in the figure, so as to shorten the cooling time and improve the production efficiency.

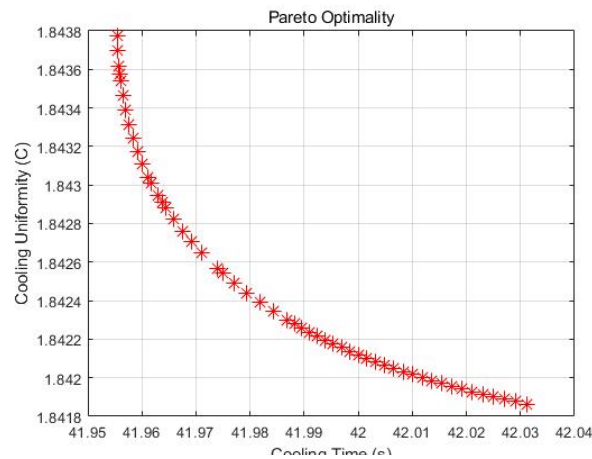


Figure 17 Pareto optimal solutions set of 500 generations of evolution

Similarly, NSGA-II on the objective functions of DOE-1 and DOE-2 algorithm optimization, the unique optimal solution of multi-objective optimization is obtained, as shown in Table 29. In order to verify the effectiveness of the optimized conformal cooling channel, software is used to model and simulate the optimized design variables, where DOE-3 with $d = 12.5$ mm, $l = 24$ mm, $s = 18$ mm, the simulation results are shown in Table 30, compared with the simulation results of the optimized conformal cooling channel, it can be seen that the optimization has

effectiveness.

Table 29 The optimal solution and optimal result after evolution

| Parameter | d/mm | l/mm | s/mm | $Obj1/S$ | $Obj2/^\circ C$ |
|-----------|--------|--------|--------|----------|-----------------|
| DOE-1 | 4 | 8 | 6 | 5.5 | 0.45 |
| DOE-2 | 8 | 16 | 12 | 17.11 | 0.4 |
| DOE-3 | 12.5 | 24 | 18 | 42 | 1.84 |

Table 30 Optimization results and simulation results

| Result | DOE-1 | | DOE-2 | | DOE-3 | |
|----------------------|-------|----------------|-------|----------------|-------|----------------|
| | y_t | $y_{\Delta t}$ | y_t | $y_{\Delta t}$ | y_t | $y_{\Delta t}$ |
| Optimization Results | 5.50 | 0.45 | 17.11 | 0.4 | 42 | 1.8 |
| Simulation results | 5.42 | 0.56 | 17.20 | 0.43 | 43.7 | 1.79 |

The significance of the factors affecting the cooling effect was screened by orthogonal test, and the optimized variables were determined to be the section size of the water channel, the distance between the water channels and the distance from the water channel to the cavity.

Using the response surface method to design conformal cooling channels for products with different wall thicknesses, the response regression model of cooling time and product cooling uniformity was established, and the relationship between cooling time and product cooling uniformity and the diameter of the cooling channel and cooling channel was obtained. The functional relationship between the spacing and the distance from the cooling channel to the cavity.

The objective functions of DOE-1 and DOE-3 were optimized by using NSGA-II algorithm, obtained the unique optimal solution of DOE-1 and DOE-2, obtained Pareto solution set of DOE-3, i.e., optimal design

parameters for different wall thicknesses. Compared with the optimized simulation results, the optimized results are reliable and applicable.

6 DESIGN SPECIFICATIONS AND EXAMPLE VERIFICATION OF CONFORMAL COOLING CHANNELS

After optimizing the design of the conformal cooling channels in the previous article, we obtained the quantitative relationship between the design variables and the cooling time and product cooling uniformity, as well as the optimal Pareto Superior frontier solution. This chapter aims at different types of product structures, according to the optimal design parameters proposed in the previous chapter, combined with engineering practice and engineering applications, proposes appropriate conformal cooling channel design specifications, and conducts product example verification.

6.1 Design specifications for conformal cooling channels

When designing cooling channels, complex plastic parts are usually decomposed into multiple simple geometric features, cooling channel design is performed for each regional feature, and then the cooling channels of all feature units are combined to form the cooling system of the entire plastic part. Considering the cost of mold manufacturing, the conformal cooling channels printed by metal 3D are usually combined with traditional linear cooling channels in actual production. Therefore, conformal cooling water channels are generally used in the curved surface feature area of the product, or the local deep cavity area where the traditional cooling method is not easy to cool, and the moving mold side

where the mold ejection mechanism is too complicated. The shape of the product is diverse, the structure of the mold is complex, and the layout of the cooling channel is usually limited. It is often impossible to design the cooling channel according to the ideal design variables. Moderate adjustment.

The design of the conformal cooling water channel should take into account four factors: the geometric shape of the product, the feasibility of the length and diameter of the water channel, the pressure drop change of the cooling liquid, and the manufacturing difficulty of channel printing. According to the previous experimental comparison and optimization analysis, combined with the special structure and manufacturing method of the conformal cooling channel, the following basic requirements should be followed in the design process of the conformal cooling channel:

1. The distance between the cooling channel and the surface of the mold cavity: when the product wall thickness is uniform, the conformal cooling channel and the mold cavity wall must always maintain the same distance. Closer to ensure that the mold temperature is as uniform as possible.

2. Cooling channel length: When the cooling channel is arranged in series, the length of the cooling channel should not be too long. One is that the turbulent state of the coolant cannot be guaranteed to prevent the pressure drop of the coolant from being too large; the other is that the excessively long cooling channel cannot take the heat out of the mold in time, which will cause the temperature of the coolant to rise and cause non-uniform cooling; at the same time, for small The longer the diameter of the water channel, the harder it is to remove the powder impurities in the channel after the printing job is completed, which increases the difficulty of insert manufacturing.

3. Cooling channel arrangement: Since the cooling effect of the cooling channel arranged in series is better than that of the parallel arrangement, for general curved surface products, the cooling channel arrangement in series or the parallel arrangement of multiple cooling channels with multiple water inlets is preferred.

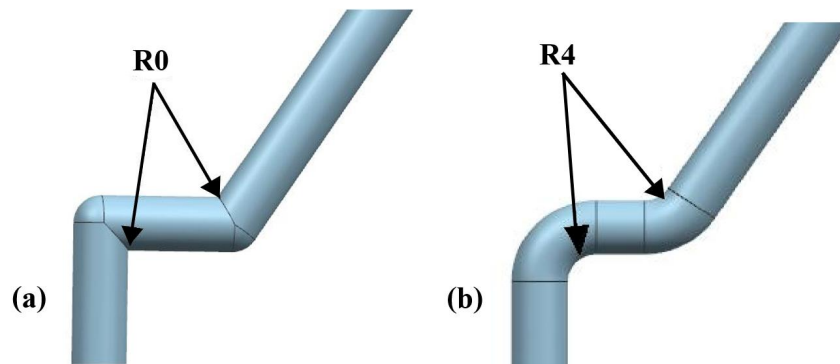


Figure 18 Design of connection part of cooling channel

- (a) Sharp corner design for cooling channel curves
- (b) Rounded corner design for cooling channel curves

4. Cooling channel connection parts: The conformal cooling channel should be designed as smooth as possible, avoiding sharp bends and right-angle bends, so that the coolant can flow under uniform pressure and speed.

5. Cross-sectional area of the cooling channel: When the cooling channel is processed by drilling, the cross-sectional area of the cooling channel remains unchanged. Similarly, for the series conformal cooling channel, the cross-sectional area of the cooling channel should remain unchanged, so that the cooling liquid passing through the cooling channel has a uniform flow rate and pressure; for the parallel conformal cooling channel, the cross-sectional area of the main cooling channel should be greater than or equal to The sum of the cross-sectional areas of each water distribution channel ensures uniform flow of water and reduces the probability of warping and deformation.

At the same time, according to the previous optimization analysis

results, combined with different types of mold structures and product features, the following design specifications for conformal cooling water channels for different feature areas and different types of products are proposed:

(1) Thin products with curved surface features

In actual production, the shape of shell-shaped products with curved surface features is often relatively flat. When there is no complex feature structure such as side holes or grooves, the product is usually molded by dynamic and static molds. At this time, the design of the cooling channel usually needs to focus on the release. The complexity of the mold mechanism, the curvature of the product surface and the distance from the cooling channel to the cavity. And the curved surface where the center line of the conformal cooling channel is located should be obtained by offsetting the product surface.

Table 31 Design parameters of conformal cooling channel for curved shell products under ideal arrangement

| wall thickness/mm | d/mm | l/mm | s/mm |
|-------------------|--------|--------|--------|
| 0-2 | 4 | 8 | 6 |
| 2-4 | 8 | 16 | 12 |
| 4-6 | 12.5 | 24 | 18 |

When the cooling channel cannot be ideally arranged according to the optimal parameters due to the existence of the ejection mechanism, the cooling channel should try to offset the product surface by the minimum distance while bypassing the ejector mechanism, so that the distance from the cooling channel to the cavity is the smallest at the same time, moderately adjust the diameter of the cooling channel and the distance between adjacent cooling channels. In order to ensure the strength and service life of the mold, the distance from the cooling channel wall to the cavity walls, the distance between adjacent cooling channel walls and the

cooling channel to the thimble hole

6.2 Cooling system design and cooling simulation based on UG and Moldflow

6.2.1 Establishment of finite element model

Meshing the plastic part is a primary process. Moldflow offers three types of meshing, including mid-plane meshing, double-layer meshing, and 3D meshing. Among these options, the mid-plane mesh model is particularly suitable for injection molded products with small and uniform thicknesses, simple structural distribution, and various locations of thickness distribution. Additionally, this type of meshing results in a relatively low number of meshes after the division process. A double-layer mesh model is a widely-used option in Moldflow, allowing for simulation of both the top and bottom of the melt flow. By using this model, injection molding processes can be accurately simulated to yield high-quality mesh and faster processing times. As a result, it is an effective tool for optimizing the structural and mold design of plastic parts, leading to improved simulation results. The three-dimensional model of the product is depicted in Fig. 19. The maximum thickness of this product is 2.11 mm, and the average thickness is less than 2 mm.

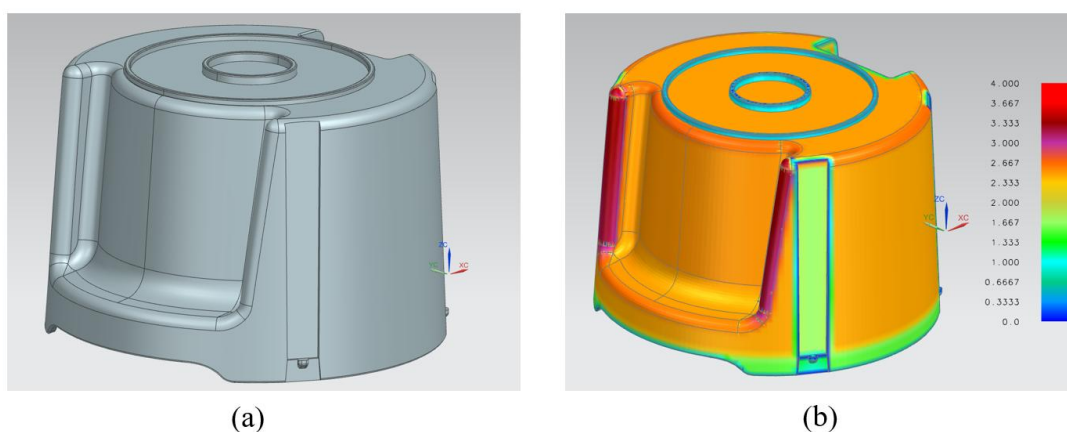


Figure 19 Model of plastic part and measurement of the wall thickness

Meshing the plastic part using a 3D mesh model in Moldflow is an effective way to accurately simulate the injection process in the entire 3D space, allowing for a realistic representation of the filling process. Since the outer surface of the plastic part typically has a complex structure with unevenly distributed wall thickness, a 3D mesh model is necessary. The edge length of the mesh is primarily determined by the thickness of the plastic part, the fit quality of the mesh, and the shape accuracy of the plastic part. Generally, it is 1.5~2 times the thickness of the plastic part to ensure the analysis accuracy.

6.2.2 Moldflow cooling analysis type selection

The cooling process of injection mold is a three-dimensional transient heat transfer process, and the transient temperature of the mold surface varies periodically with the injection process. In practical engineering applications, it is generally reduced to a steady-state heat transfer process. Among the cooling analysis types in Moldflow, the main types include BEM cooling analysis and FEM cooling analysis.

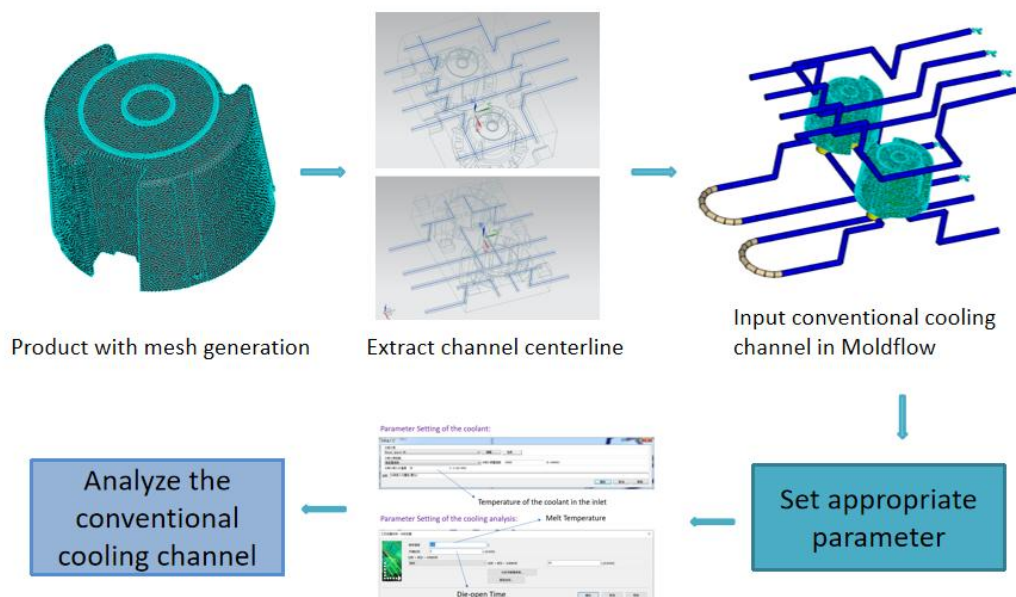


Figure 20 Procedure of the analysis and simulation of the part by Moldflow

The Boundary Element Method (BEM) is a numerical approach used to analyze the cooling process of plastic parts in injection molding. BEM cooling analysis is utilized to determine the average temperature of the plastic part during the steady state or the entire molding cycle. In the cooling simulation, the boundary element method cooling analysis can easily change the position of the cooling channel, get the effect of the position of the cooling channel on the cooling effect of the mold, and optimize the design of the cooling channel. FEM cooling analysis calculates both steady-state and transient temperatures of the mold by the finite element method. In the steady state, the mold temperature is uniform, while in the transient state, the mold temperature varies with time.

Finite Element Method (FEM) cooling analysis employs two main methods to analyze transient temperatures in molds: intra-cycle transient and transient after the start of production. Intra-cycle transient analysis simulates temperature fluctuations in the mold during a single cycle and calculates the deviation of the mold temperature from the cycle's average value. This analysis helps to identify and mitigate potential temperature-related issues during production. The other method, transient after the start of production, evaluates temperature changes in the mold after production has begun. These two types of analyses are commonly used in finite element cooling analysis to comprehensively understand and optimize the temperature dynamics of molds during different phases of production.

The post-start transient calculates the change in mold temperature from the initial production cycle in the cold state to the time when the mold temperature stabilizes and reaches its optimal conditions, and calculates the number of cycles required for the mold to reach its optimal production conditions. In order to accurately simulate and predict the temperature

distribution of the mold cavity walls, this paper employs the FEM cooling analysis type for cooling simulation.

6.2.3 Selecting the proper type of conformal cooling channels for thin wall products

Owing to the geometric liberty afforded by rapid metal processing techniques, such as selective laser sintering and selective laser melting, the fabrication of conformal cooling channels with versatile cross-sectional profiles and geometries is feasible. Among the prevalent options, spiral-shaped conformal cooling channels are commonly deployed due to their ability to maintain near-constant coolant velocity, despite their potential for elevated pressure drop. Conversely, scaffolded conformal cooling channels and Voronoi diagram channels exhibit lower pressure drop but pose challenges in achieving uniform coolant velocities, which may result in stagnation in certain channel segments.

The impact of channel cross-section on cooling performance was investigated by Jahan et al., who found that rectangular channels demonstrated superior cooling performance. However, this type of cross-section may not fully align with the manufacturability requirements of additive manufacturing methods. On the other hand, elliptical, circular, and teardrop cross-sections are characterized by easier printability,

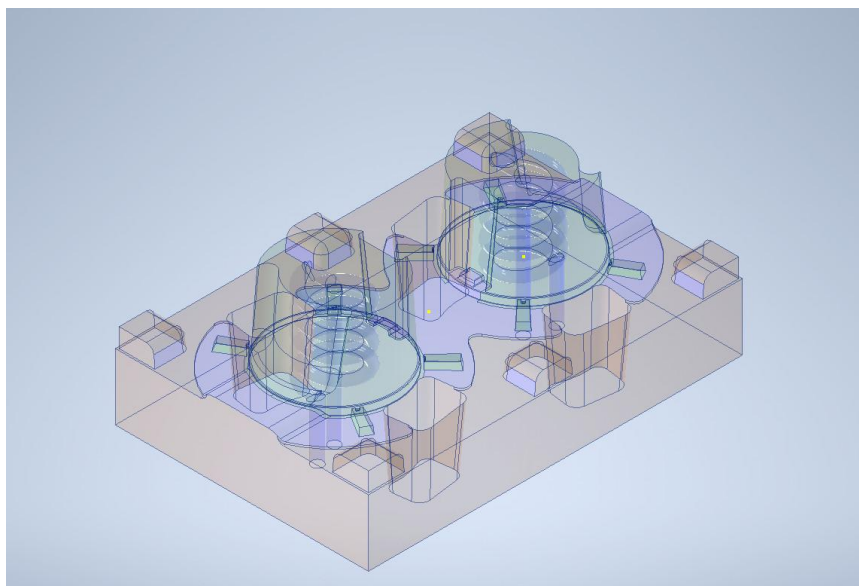


Figure 21 The model of the mold with simple spiral cooling channels

without the need for support structures and stress concentrations.

Considering the cylindrical shape of the target product, and taking into account the aspects of product shape, manufacturing cost, and feasibility of production processes, we have chosen spiral-shaped cooling channels with circular cross-sections. Fig. 21 displays the model of simple spiral-shaped cooling channels.

6.3 The design of conformal cooling channels for the products

Effective cooling channel design for injection molding often involves dividing the mold into several geometrical features, with separate channels designed and laid out for each feature. These features are then combined to form the complete cooling system for the injection molding process. In order to balance mold manufacturing and plastic part production costs, injection cooling system molds typically use a combination of straight-through and shaped cooling channels.

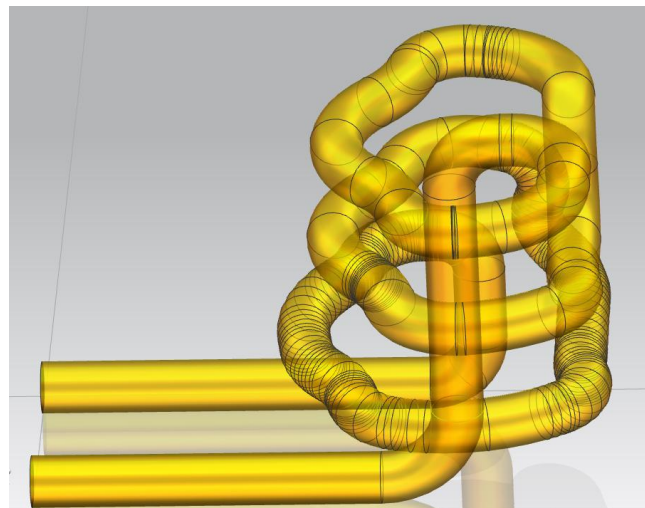


Figure 22 Local layout of the conformal cooling channel

Conformal cooling channels are mainly used for complex curved features of plastic parts or deep cavity features where conventional cooling channels cannot achieve the cooling effect. Additionally,

conformal cooling channels are often utilized for injection molds with moving parts and complex ejection systems.

6.4 The model of the mold with conventional cooling channels

The layout of cooling channels in molds is often limited by the mold's intricate surface features and complex structure. As shown in Fig. 23, a conventional channel model is shown. Obviously, the channels are all straight-drilled type. In practice, the design of cooling channels cannot always be achieved according to the ideal design scheme due to these limitations. As a result, mold designers need to have the expertise to continually modify the plastic part to match the shape, size, wall thickness, and structural characteristics of the cooling water channels. This requires a deep understanding of the manufacturing process and the ability to optimize the design of cooling channels to ensure optimal performance of the mold.

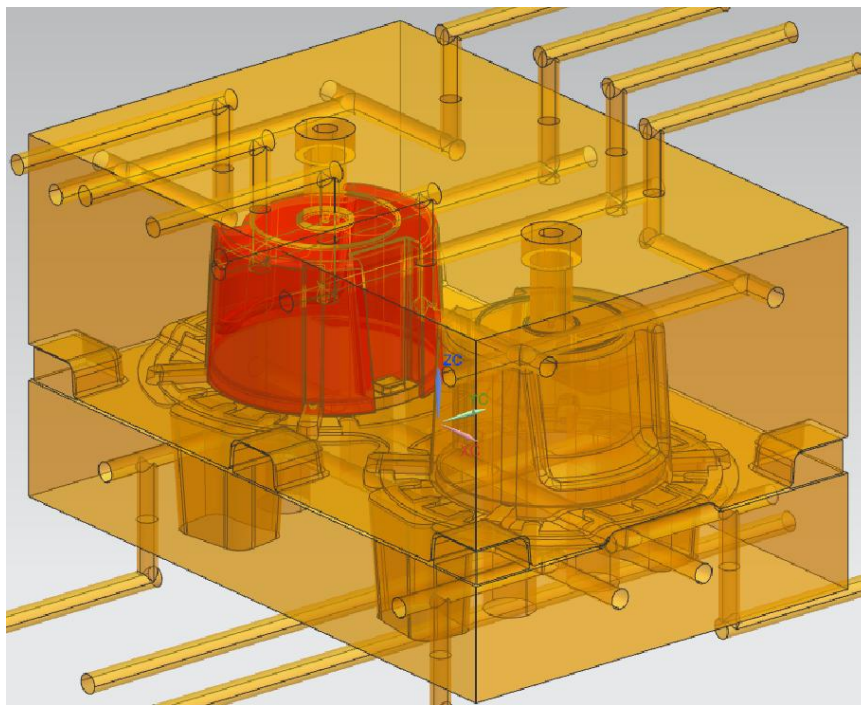


Figure 23 The model of the mold with conventional cooling channels

Cooling channel design principles and specifications are as follows. Figure 22 Local layout of the conformal cooling channel displays the local geometric configuration of conformal cooling channels, which exhibit a more complex shape that conforms closely to the shape of the product.

(1) The distance between the centerline of the cooling channel and the cavity wall is a critical consideration in mold design. When the product thickness is uniformly distributed, it is essential to maintain a consistent distance between the cooling channel's centerline and the cavity wall throughout. However, when the product thickness is unevenly distributed, it is necessary to decrease the distance between the cooling channel's centerline and the cavity wall in the thicker areas to ensure that the product cools uniformly. This is particularly important to prevent warpage and deformation and to achieve the desired product quality. Therefore, careful consideration of the cooling channel layout is crucial to achieve optimal mold performance and ensure consistent product quality.

(2) Cooling channel layout: There are two types of layout, namely series and parallel layout. When cooling channels are connected in series, the coolant flow rate remains basically unchanged, but under the complex cooling channel layout, the channel loss value and pressure drop are larger. When cooling channels are connected in parallel, the flow rate in each branch cooling channel is different, resulting in uneven cooling of plastic parts. Therefore, in order to avoid encountering the problems of the parallel connection method, the series layout method should be given priority.

(3) Cooling channel length: increasing the length of the cooling channel will increase the heat transfer area of the channel, and when using a series cooling channel in a series layout, the longer channel may

lead to the excessive pressure drop of the coolant, therefore, the channel length should not be too long.

6.5 Cooling channel design and modeling

In the injection molding process, because the traditional straight-drilled cooling channels cannot effectively cool the slider and insert it into the deep cavity of the plastic part, this can result in local heat concentration in the plastic part, ultimately affecting the overall cooling time.

Table 32 Injection molding process parameter setting

| Injection Molding Process Items | Parameter |
|--|-----------------------|
| Injection Machine Clamping Force | 150 ton |
| Injection Material | PA 66 |
| Cycle Time | 52 s |
| Mold Open and Ejecting Time | 6 s |
| Mold Close Time | 4 s |
| Injection Unit Forward | 4 s |
| Filling Time | 2 s |
| Holding Time | 3 s |
| Injection Unit Backward | 3 s |
| Cooling Time | 34 s |
| Injection Pressure | 50 kg/cm^2 |
| Holding Pressure | 60 kg/cm^2 |
| Material Temperature at Injection | 260°C |
| Material Surface Temperature at Ejection | 65°C |
| The temperature of Coolant | 20°C |
| Water Volume | Tot. 16L, Each 8L/min |
| Mold Surface Temperature at Ejection | 40°C |
| Mold Material | P20 Steel |
| Coolant Pressure | 0.2 MPa (2bar) |

6.6 Analysis and comparison of cooling results

Based on the establishment of the cooling system model, the selection of injection process parameters and the establishment of the mold gating system mentioned above, the cooling simulation was carried out for the two groups of cooling system design solutions respectively.

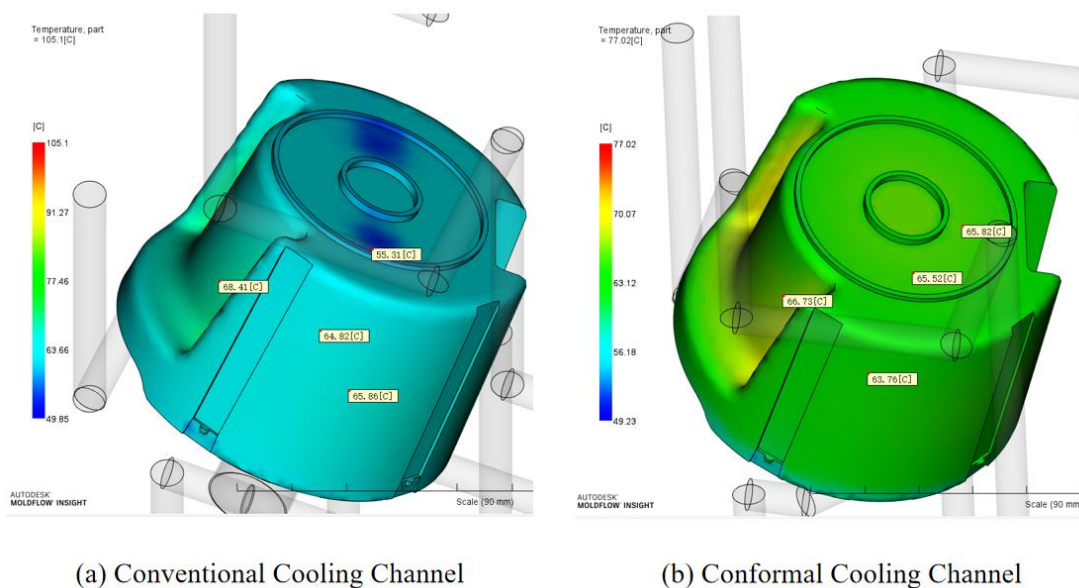


Figure 24 Simulation results for the temperature of part after the cooling process

Figure 25 Detailed temperature distribution within the part

As evident from Figure 24 Simulation results for the temperature of part after the cooling process

Figure 25 Detailed temperature distribution within the part

Simulation results for the temperature of part after the cooling process 24, the simulation results reveal that the product employing the conventional cooling system attains a maximum temperature of 105.1°C at the end of

the cooling process, whereas the product incorporating the conformal cooling channels exhibits a significantly lower maximum temperature of 77.02 °C. The cooling system with conformal cooling channels demonstrates higher efficiency in the cooling process compared to the traditional cooling system, leading to a more uniform and lower temperature distribution of the plastic parts.

Fig. 25 also presents the detailed temperature distribution within the part. Based on the findings obtained from the simulation results, it is apparent that the utilization of conformal cooling channels in the product design results in lower temperatures compared to conventional cooling channels, accompanied by a more homogeneous temperature distribution.

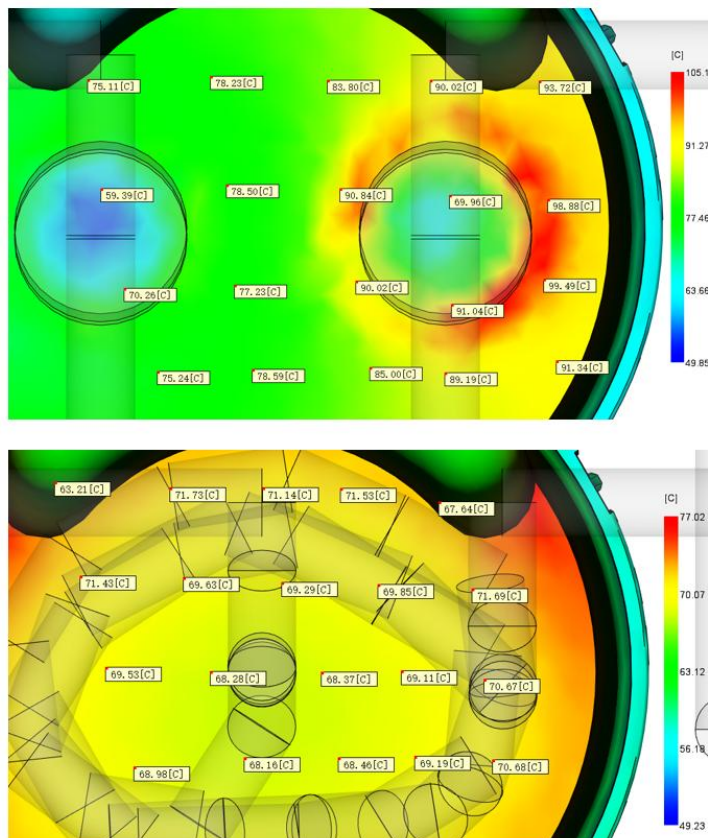


Figure 25 Detailed temperature distribution within the part

Figure 26 Time to reach ejection temperature of part
Figure 25 Detailed temperature distribution within the part

The implementation of conformal cooling channels in the product design leads to improved heat transfer efficiency from the product surface to the cooling medium. Furthermore, the arrangement of these channels has the potential to enhance the uniformity of temperature distribution on the product surface by mitigating the occurrence of hot spot areas, which are localized regions with elevated temperatures. The strategic placement of cooling channels in proximity to these hot spot areas facilitates effective heat dissipation, resulting in reduced temperature gradients and enhanced uniformity of temperature distribution.

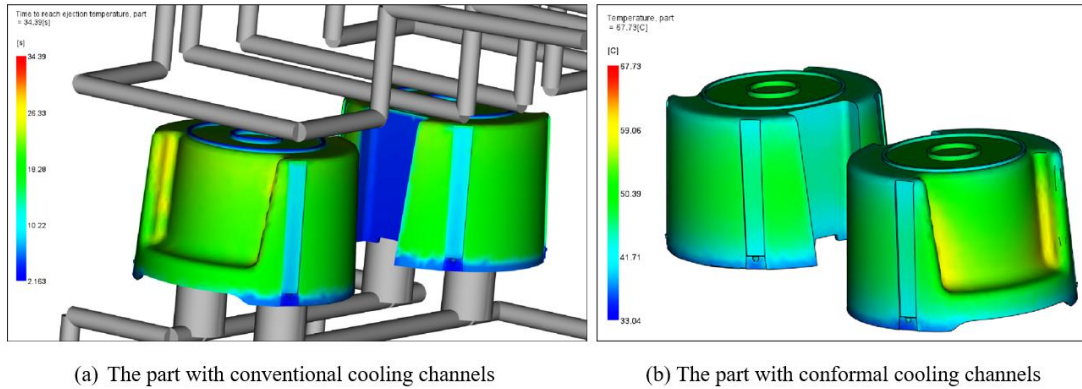


Figure 26 Time to reach ejection temperature of part

Figure 27 Distinct time for various sections of the part to reach the ejection temperature

Figure 15 Time to reach ejection temperature of part
Figure 16 Distinct time for various sections of the part to reach the ejection temperature
Figure 26 Time to reach ejection temperature of part

From Fig. 26, it is evident that the time required to reach the ejection temperature using conventional cooling channels is 34.39 seconds, whereas the time using conformal cooling channels is reduced to 24.19 seconds, resulting in a significant reduction in cooling time by 10.20 seconds. This reduction in cooling time underscores the superior performance of conformal cooling channels over conventional cooling channels in achieving the desired ejection temperature.

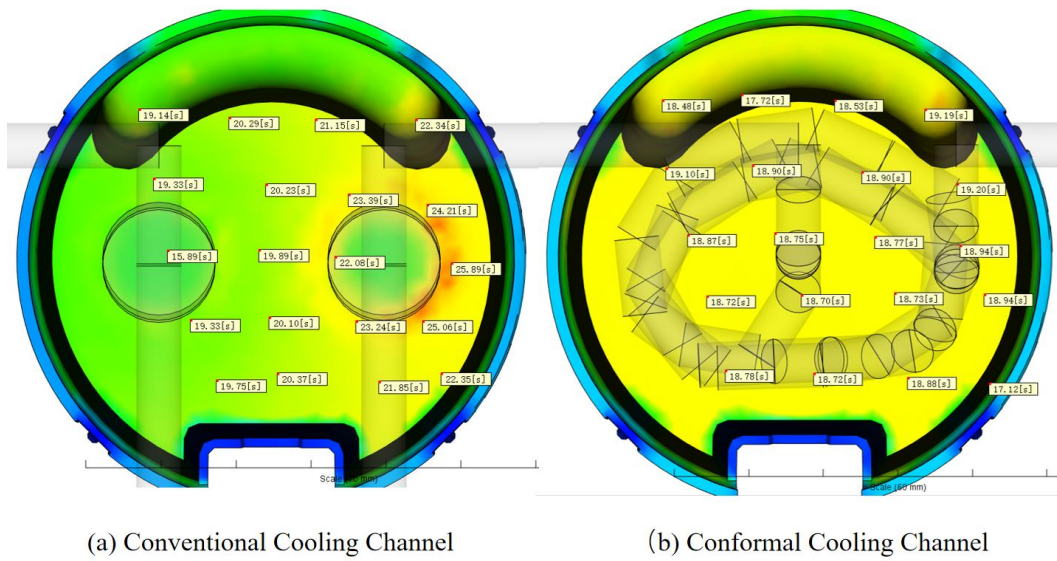


Figure 27 Distinct time for various sections of the part to reach the ejection temperature

Fig. 27Figure 27 Distinct time for various sections of the part to reach the ejection temperature

Figure 17 Time to reach ejection temperature of part Figure 18 Distinct time for various sections of the part to reach the ejection temperature showcases the distinct time required for various sections of the plastic parts to reach the ejection temperature. And the statistical data for a randomly chosen point on the surface of the simulated part. The data indicates that when utilizing conformal cooling channels, the product temperatures are significantly lower compared to conventional ducts, with a temperature reduction ranging from 11 to 28 °C. Additionally, the average time required to attain the ejection temperature is 32.29% lower with the use of conformal cooling channels as compared to conventional channels. We can calculate the cooling efficiency of the conformal cooling channel is more than 30%.

7 SUMMARY AND CONCLUSIONS

Conformal cooling channels can significantly reduce the cooling time, achieve uniform cooling and improve the quality of molded parts, especially for large-scale and complex-geometries products. Designing and optimizing conformal cooling channels for injection molding requires a complicated analysis process, optimization strategies, and appropriate computer-aided tools. This study proposes a method to optimize the cooling system to obtain the target mold temperature, and reduce the cooling time and non-uniformity of the molding temperature distribution, and increase productivity. To improve computational efficiency, analytical methods, and simulation-based methods are used successively. The relationship between the thermal behavior of the die and the cooling channel layout parameters has been carefully investigated. The feasibility of the analytical method is demonstrated by comparing the results of this method with DOE approximations. It can be concluded that the analytical method is suitable for optimizing conformal cooling channels with moderate accuracy.

REFERENCES

- [1] Adam, WB Du Preez, and J Combrinck. "Design considerations for additive manufacturing of conformal cooling channels in injection moulding tools". In: *Interim: Interdisciplinary Journal* 15.1 (2016), pp. 35–44.
- [2] BM Saifullah and SH Masood. "Finite element thermal analysis of conformal cooling channels in injection moulding". In: *Proceedings of the 5th Australasian congress on applied mechanics. Engineers Australia Brisbane, Qld. 007*, pp. 337–341.
- [3] DE Dimla, M Camilotto, and FJJOMPT Miani. "Design and optimisation of conformal cooling channels in injection moulding tools". In: *Journal of Materials Processing Technology* 164 (2005), pp. 1294–1300.
- [4] Maciej Mazur et al. "Numerical and experimental evaluation of a conformally cooled H13 steel injection mould manufactured with selective laser melting". In: *The International Journal of Advanced Manufacturing Technology* 93 (2017), pp. 881–900.
- [5] Kunayut Eiamsa-Ard and Kittinat Wannissorn. "Conformal bubbler cooling for molds by metal deposition process". In: *Computer-Aided Design* 69 (2015), pp. 126–133.
- [6] Tim Evens et al. "Experimental analysis of conformal cooling in SLM produced injection moulds: Effects on process and product quality". In: *AIP Conference Proceedings*. Vol. 2055. 1. AIP Publishing LLC. 2019, p. 070017.
- [7] AJ Norwood et al. "Analysis of cooling channels performance". In: *International Journal of Computer Integrated Manufacturing* 17.8 (2004), pp. 669–678.
- [8] Marian Blaško, Viktor Tittel, and Martin Ridzoň. "Cae Analysis Of Conformal Cooling Application–Case Study". In: *International Journal of Engineering* 10 (2012).
- [9] Hong-Seok Park and Xuan-Phuong Dang. "Development of a smart plastic injection mold with conformal cooling channels". In: *Procedia Manufacturing* 10 (2017), pp. 48–59.
- [10] Yingming Zhang et al. "Automatic design of conformal cooling channels in injection molding tooling". In: *IOP Conference Series: Materials Science and Engineering*. Vol. 307. 1. IOP Publishing. 2018, p. 012025.
- [11] Ognjen Tuteski and Atanas Kočov. "Conformal cooling channels in injection molding tools–design considerations". In: *Machines. Technologies. Materials.*

12.11 (2018), pp. 445–448. Version June 2, 2023 submitted to Journal Not Specified 22 of 22

- [12]Khurram Altaf and Ahmad Majdi bin Abdul Rani. “Numerical study of profiled conformal cooling channels for cooling time reduction in injection mould tools”. In: *International Journal of Engineering Systems Modelling and Simulation* 7.4 (2015), pp. 230–237.
- [13]Gerald R Berger et al. “Efficient cooling of hot spots in injection molding. A biomimetic cooling channel versus a heat-conductive mold material and a heat conductive plastics”. In: *Polymer Engineering & Science* 59.s2 (2019), E180–E188.
- [14]Kamal Kumar Agrawal et al. “Computational fluid dynamics simulation based comparison of different channel layouts in an EATHE system for cooling operation”. In: *Journal of Thermal Science and Engineering Applications* 11.5 (2019).
- [15]Jae Hyuk Choi et al. “Study on an optimized configuration of conformal cooling channel by branching law”. In: *Engineering Systems Design and Analysis*. Vol. 45837. American Society of Mechanical Engineers. 2014, V001T06A007.
- [16]G Venkatesh and Y Ravi Kumar. “Thermal analysis for conformal cooling channel”. In: *Materials Today: Proceedings* 4.2 (2017), pp. 2592–2598.
- [17]Suchana A Jahan et al. “Implementation of conformal cooling & topology optimization in 3D printed stainless steel porous structure injection molds”. In: *Procedia Manufacturing* 5 (2016), pp. 901–915.
- [18]Suchana A Jahan and Hazim El-Mounayri. “Optimal conformal cooling channels in 3D printed dies for plastic injection molding”. In: *Procedia Manufacturing* 5 (2016), pp. 888–900.
- [19]Dong-Gyu Ahn, Seung-Hwa Park, and Hyung-Soo Kim. “Manufacture of an injection mould with rapid and uniform cooling characteristics for the fan parts using a DMT process”. In: *International Journal of Precision Engineering and Manufacturing* 11 (2010), pp. 915–924.
- [20]Xuan-Phuong Dang and Hong-Seok Park. “Design of U-shape milled groove conformal cooling channels for plastic injection mold”. In: *International Journal of precision engineering and manufacturing* 12 (2011), pp. 73–84.
- [21]Ismet Ilyas et al. “Design and manufacture of injection mould tool inserts produced using indirect SLS and machining processes”. In: *Rapid Prototyping Journal* 16.6 (2010), pp. 429–440.
- [22]ABM Saifullah and Syed H Masood. “Cycle time reduction in injection moulding with conformal cooling channels” In: *Proceedings of the International Conference on Mechanical Engineering*. 2007, pp. 29–31.
- [23]Alban Agazzi et al. “Optimal cooling design in injection moulding process—A new approach based on morphological surfaces”. In: *Applied Thermal Engineering* 52.1 (2013), pp. 170–178.
- [24]Natti S Rao et al. “Optimization of cooling systems in injection molds by an easily applicable analytical model”. In: *Journal of reinforced plastics and composites* 21.5 (2002), pp. 451–459.

- [25]SJ Park and TH Kwon. "Optimal cooling system design for the injection molding process". In: Polymer Engineering & Science 38.9 (1998), pp. 1450–1462.
- [26]Jack Philip Holman. Heat transfer. McGraw Hill Higher Education, 2010.
- [27]Natti S Rao and Günter Schumacher. Design formulas for plastics engineers. Carl Hanser Verlag GmbH Co KG, 2014.
- [28]Georg Menges, Walter Michaeli, and Paul Mohren. How to make injection molds. Carl Hanser Verlag GmbH Co KG, 2013.